Perfluorocyclohexenyl (PFCH) Aromatic Ether Polymers from Perfluorocyclohexene and Polycyclic Aromatic Bisphenols

Ganesh Narayanan, Behzad Faradizaji, Karl M. Mukeba, Ketki E. Shelar, Maleesha DeSilva, Amanda Patrick, Bruno Donnadieu, and Dennis W. Smith., Jr.*

Department of Chemistry and The Marvin B. Dow Advanced Composites Institute, Mississippi State University, Starkville, MS 39759, USA.

---

* To whom correspondence should be addressed:

Dennis W. Smith, Jr., Ph.D.

Department of Chemistry,
Mississippi State University, MS-39762,
Email: dsmith@chemistry.msstate.edu,
Ph: +1-662-325-7813

Table of Contents

General Experimental Methods.

All the reactions were carried out in oven-dried (120 °C) glassware under argon atmosphere, unless otherwise stated. Acenapthenequinone (cat#102191000), triethylsilane (cat#AO362371), trifluoromethanesulfonic acid (cat#A0355787) were purchased from Acros organics, NJ, USA, and phenanthrene-9,10-dione(cat#23173), tetrahydrofuran (THF) (cat#0099898), trifluoroacetic acid (cat#001271), methanesulfonic acid (cat#152800) were purchased from Oakwood chemicals, SC, USA. Other reagents utilized in this study: chloroform (cat # C2432), 1-dodecanethiol (cat#08225AD), *N,N*-dimethylformamide (DMF) (cat # 227056), toluene (cat#179418), triethylamine (cat#A0393087) were purchased from Sigma-Aldrich, St. Louis, MO, USA. The remainder of the chemicals, dichloromethane, hexanes (cat#H292-20), methanol (cat#A456-4), phenol (cat#A92-500), acetonitrile (cat# A955-4)), were obtained from Fisher Scientific, NH, USA. Finally, fluoro-olefin monomer, decafluorocyclohexene (cat# 1400-2-10), was obtained from Synquest labs, FL, USA. De-ionized water (bulk resistivity of 14 mΩ cm) was obtained from in-house water purification system based on a reverse osmosis process.

Materials Characterization.

Fourier Transform Infrared Spectroscopy (FTIR) experiments were conducted using an Agilent Cary 630 spectrophotometer with a diamond crystal ATR sample head between the wavelengths 4000 to 400 cm^{-1}. The experiments were carried at a resolution of 2 cm^{-1}, and one hundred twenty-eight scans were carried out for each sample.

Nuclear magnetic resonance (NMR) experiments (^{1}H, ^{19}F, ^{13}C, NOESY, HSQC, HBMC (^{1}H-^{13}C)) were measured on a Bruker AVANCE III 500 and 300 MHz instrument. For as-synthesized bisphenols, methanol-d_4 (CD_3OD), and DMSO-d_6 were used as solvent. Similarly, for polymers (homo- and copolymers) (**P1**-**P6**), chloroform-d ($CDCl_3$) was used as a solvent for NMR experiments, and all chemical shifts are reported in parts per million (δ ppm).

High resolution mass spectrometric (HR-MS) experiments were carried out on a Bruker UHPLC microTOF-Q II HR-MS via injection and ionization of monomers (**M1-M4** in methanol) using atmospheric pressure chemical ionization (APCI) technique. The data was obtained within mass accuracies of 1-10 ppm RMS error and at resolution greater than 17500 full width at height maximum (FWHM).

Single crystal X-ray diffraction data of **M2** and **M4** with approximate dimensions of 0.131 x 0.168 x 0.299 mm^3 (**M2**) and 0.086 x 0.203 x 0.510 (**M4)**, respectively, were obtained from a Bruker AXS D8 Venture equipped with a Photon 100 CMOS active pixel sensor detector using copper monochromatized X-ray radiation (λ = 1.54178 Å). The

data were processed by integrating the frames with the aid of the Bruker SAINT software using a narrow-frame algorithm and absorption-induced effects were corrected using a multi-scan method implemented in the SADABS program. The ratio of minimum to maximum apparent transmission for **M2** was 0.867. The calculated minimum and maximum transmission coefficients (based on crystal size) were 0.8310 and 0.9210. On the other hand, the ratio of minimum to maximum for **M4** was 0.810 and calculated minimum and maximum transmission coefficients (based on crystal size) were 0.7300 and 0.9460. The structures of **M2** and **M4** were solved and refined using the Bruker SHELXT- Software Package, using the space group P-1, with Z = 2 for the formula unit, $C_{24}H_{16}O_2$ **(M2)** and $C_{28}H_{26}O_4$ (**M4**). Refinement of the structure **M2** was carried out by least squares procedures on weighted F^2 values using the SHELXL-2016/6 included in the APEX3 v2018, 1.0, AXS Bruker program. Hydrogen atoms, which were localized on difference Fourier maps were then introduced in the refinement as fixed contributors in idealized geometry with an isotropic thermal parameter fixed at 20 % higher than the carbons atoms they were connected. In **M4**, the asymmetric unit was built with two independent molecules labelled: A and B. Refinement of the structure **M4** as mentioned above for **M2.**

Differential scanning calorimetric (DSC) experiments were conducted to study the thermal order-disorder events of the homo- and co-polymers using a TA Q20 V4. DSC instrument. Approximately, 3 to 5 mg of the polymer was placed in TA low-mass aluminum pan, sealed, and a heat–cool-heat cycle (4 heating and 4 cooling cycles) was employed between the temperatures of 0–300 °C at a scanning rate of 10 °C/min. Between the cycles, the pans were

isothermally held at 300 °C and at 0 °C for 3 mins. The raw data was extracted using TA universal analysis software V4.5a. For clarity, the data were standardized using Minitab® 18, and the plots were created using OriginPro 2018.

Thermal degradation patterns of the polymers were carried out on small samples (5 to 10 mg) using a TA Q50 V20 Thermogravimetric analyzer (TGA) instrument over the temperature range 30–800 °C, at a heating rate of 10 °C/min. The experiments were carried out under both nitrogen and air, and TA universal analyses software was used to analyze the degradation patterns, and the data was exported for further processing using OriginPro 2018.

Molecular weight measurements based on gel permeation chromatography (GPC) data were collected using a TOSOH EcoSEC HLC-8320 gel permeation chromatograph at 30 °C, equipped with TSK gel super H-RC columns (6 mm internal diameter, 15 cm long, particle size 4 μm). HPLC grade tetrahydrofuran (THF) was used an eluting solvent at a flow rate of 0.7 mL/min. The molecular weights (M_n, M_w, and M_z) were obtained by calibrating against polystyrene standards based on the retention times monitored by UV detector (λ= 254 nm).

Synthesis of 2-bis(4-hydroxyphenyl)acenaphthene-1-(2H)-one (**M1**).

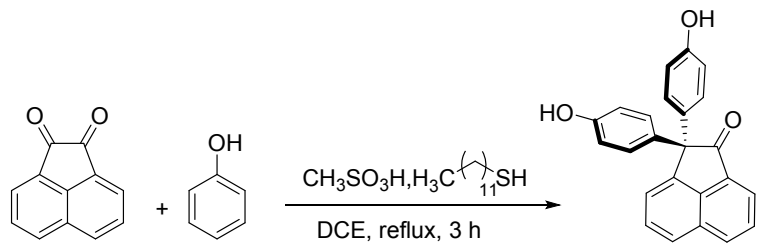

8 **M1**

Compound **M1** was synthesized based on a previously reported protocol with modifications[S1]. To a mixture of acenaphthoquinone (3.00 g, 16.5 mmol), phenol (9.29 g, 98.7 mmol), and 2 mL of 1-dodecanethiol was added 50 mL dichloroethane in a 250 mL round-bottom flask, equipped with magnetic stir bar, and fitted with condenser and rubber septa. 2 ml of methanesulfonic acid was added under argon atmosphere. The reaction mixture was stirred under reflux condition for 3 h before it was allowed to cool to rt. The precipitate was subsequently filtered and washed with dichloromethane (3 × 100 mL) and water (2 × 100 mL), and air-dried for 8 h to give **M1** (5.11 g, 14.5 mmol, 88% yield) as a white solid: mp 263.28 °C; IR 3600–3000, 1694, 1592, 1506, 1431, 1368, 1216, 1176, 1112, 1003, 815, 783, 640, 545, 519, and 490 cm^{-1}; ^{1}H NMR (CD_3OD, 500 MHz,) δ 8.22 (1 H, d, J = 8.2 Hz), 7.98 (1 H, d, J = 6.7 Hz), 7.90 (1 H, d, J = 8.2 Hz), 7.80 (1 H, dd, J = 7.9, 7.0 Hz), 7.67 (1 H, dd, J = 8.5, 7.0 Hz), 7.42 (1 H, d, J = 6.7 Hz), 7.00 (4 H, d, J = 8.9 Hz), 6.67 (4 H, d, J = 8.9 Hz); ^{13}C NMR (CD_3OD, 125 MHz,) δ 207.0, 157.7, 145.4, 142.3, 135.1, 133.4, 130.9, 129.9, 124.0, 123.6, 116.2, 67.8; HRMS (ACPI) m/z: $[M]^+$ Calcd for $C_{24}H_{16}O_3$ 352.1099; Found 352.1087

Synthesis of 4,4'- (1,2-acenaphthylenediyl)bisphenol (**M2**).

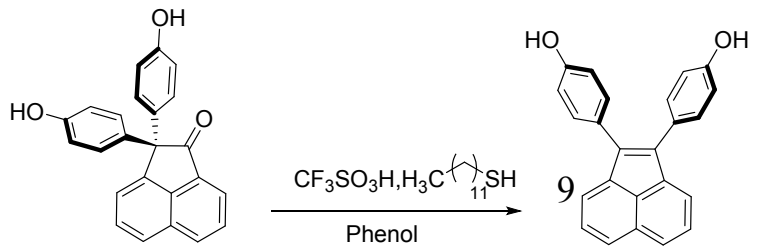

M2

In a 50 mL round-bottom flask, 0.35 g (0.99 mmol) of 2-bis(4-hydroxyphenyl)acenaphthene-1-(2H)-one (**M1**), phenol 0.73 g (7.8 mmol), 1-dodecanethiol 0.085 g (0.42 mmol) were added and equipped with magnetic stir bar, and fitted rubber septa. The flask was flushed with argon for 5 min and the mixture heated at 80 °C under stirring. Then, 2 mL of triflic acid was added via syringe and stirred for 8 hours at 80 °C. After 8 h of reaction, the mixture was cooled to rt and subsequently diluted with distilled water (100 mL). The reaction mixture was extracted by ethyl acetate (3 × 50 mL). The combined organic layer was washed with distilled water (2 × 50 mL). The organic layer was dried over sodium sulfate and concentrated in vacuo. The residue was further purified by column chromatography (silica gel/ toluene: ethyl acetate = 1:12 to 1:8) and recrystallized from dichloromethane to produce **M2** (140 mg, 0.42 mmol, 42% yield) as a orange solid: mp 252.51 °C; IR: 3480-3040, 1594, 1546, 1472, 1426, 1363, 1216, 1098, 1011, 820, 749, 688, 579, 504, and cm^{-1}; ^{1}H NMR (CD_3OD, 300 MHz,) δ 7.79 (2 H, d, J = 8.1 Hz), 7.62 (2 H, d, J = 7.0 Hz), 7.54 (2 H, t, J = 7.4 Hz), 7.24 (4 H, d, J = 8.6 Hz), 6.80 (4 H, d, J = 8.8 Hz); ^{13}C NMR (CD_3OD, 125 MHz,) δ 158.0, 141.9, 138.2, 132.4, 129.9, 128.90, 128.89, 128.1, 127.9, 124.3, 116.4; HRMS (ACPI) m/z: $[M]^+$ Calcd for $C_{24}H_{16}O_2$ 336.1150; Found 336.1160

.Synthesis of 10,10-bis(4-hydroxyphenyl)phenanthren-10

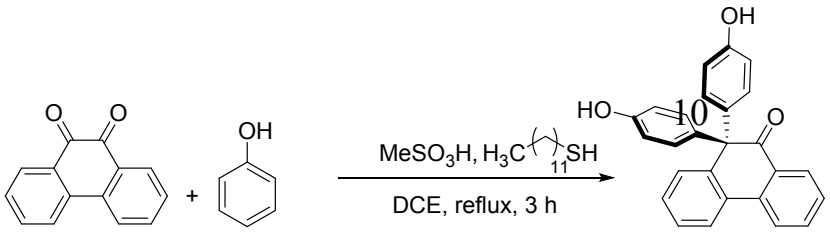

M3

9(10H)-one **(M3)**.

Compound **M3** was synthesized based on a previously reported procedure for synthesizing compound **M1.** To a mixture of phenanthrene-9,10, dione (10.0 g, 48.0 mmol), phenol (27.08 g, 287.7 mmol), and 2 mL of 1-dodecanethiol was added 250 mL dichloroethane in a 1 L round-bottom flask, equipped with magnetic stir bar, and fitted with condenser and rubber septa. 3 ml of methanesulfonic acid was added under argon atmosphere. The reaction mixture was stirred under reflux condition for 3 h resulting in the precipitation of **M3** before it was allowed to cool to rt. The precipitate was subsequently filtered and washed with dichloromethane (5 × 100 mL) and water (4 × 100 mL), and air-dried for 8 h to give **M3** (15.62 g, 41.3 mmol, 86% yield) as a white solid: mp 262.51°C; IR 3515–3270, 1663, 1589, 1504, 1437, 1357, 1298, 1227, 1175, 1114, 1013, 870, 825, 772, 734, 669, 637, 599, 569, and 519 cm^{-1}; ^{1}H NMR (CD_3OD, 500 MHz,) δ 8.10 (1 H, d, J = 7.9 Hz), 8.02 (1 H, d, J = 7.9 Hz), 7.83 (1 H, d, J = 7.7 Hz), 7.62 (1 H, t, J = 7.6 Hz), 7.44 (1 H, t, J = 7.6 Hz), 7.36 (1 H, t, J = 7.5 Hz), 7.26 (1 H, t, J = 7.5 Hz), 6.74 (1 H, d, J = 7.9 Hz), 6.72–6.67 (4 H, m), 6.67–6.59 (4 H, m); ^{13}C NMR (CD_3OD, 125 MHz,) δ 203.0, 157.9, 143.3, 138.2, 135.5, 134.0,

133.0, 132.8, 132.5, 131.8, 129.7, 129.5, 129.1, 128.8, 125.5, 124.3, 115.9, 68.6; HRMS (ESI/Q-TOF) m/z: $[MH]^+$ Calcd for $C_{26}H_{18}O_3$ 379.1334 ; Found 379.1328.

Synthesis of 4,4'-(phenanthrene-9,10-diyl)diphenol (**M4**).

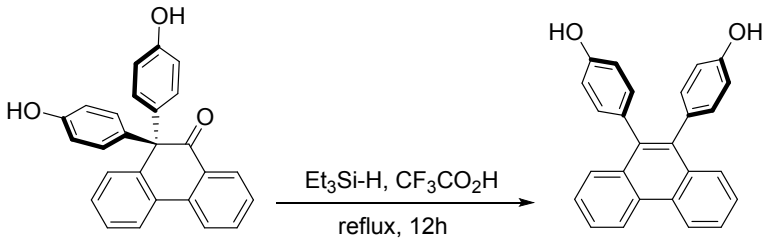

M4

To a 100 mL round-bottom flask were added **M3** (10.0 g, 26.43 mmol), 50 mL of trifluoroacetic acid, and triethylsilane (3.69 g , 31.72 mmol). The flask was equipped with magnetic stir bar, fitted with condenser and rubber septa, and flushed with argon. The reaction mixture was stirred at reflux for 12 h before it was cooled to rt. The precipitate was filtered and washed with dichloromethane (3 × 50 mL), and air-dried for 2 h to give **M4** (7.86 g, 21.7 mmol, 82% yield) as a white solid: mp 311.59 °C; IR 3640–3086, 1701, 1654, 1609, 1507, 1487, 1420, 1355, 1206, 1101, 1045, 1015, 886, 854, 812, 758, 724, 625, 585, 546, 509, and 426 cm^{-1}; ^1H NMR (CD_3OD, 500 MHz,) δ 8.82 (2 H, d, J = 8.2 Hz), 7.62 (2 H, t, J = 7.6 Hz), 7.56 (2 H, d, J = 7.6 Hz), 7.46 (2 H, t, J = 7.6 Hz), 6.93 (4 H, d, J = 8.5 Hz), 6.69 (4 H, d, J = 8.5 Hz); ^1H NMR (DMSO-d_6, 500 MHz,) δ 9.33 (2 H, s), 8.91 (2 H, d, J = 8.2 Hz), 7.67 (2 H, ddd, J = 8.2, 6.9, 1.4 Hz), 7.53 (2 H, td, J = 8.0, 0.6 Hz), 7.47 (2 H, dd, J = 8.3, 1.0 Hz), 6.91 (4 H, d, J = 8.6 Hz), 6.67 (4 H, d, J =

8.6 Hz); ^{13}C NMR (CD_3OD, 125 MHz,) δ 157.0, 138.8, 133.9, 133.4, 132.5, 131.5, 128.9, 127.6, 127.4, 123.7, 115.7; HRMS (ACPI) m/z: $(M)^+$ Calcd for $C_{26}H_{18}O_2$ 363.1385; Found 363.1391

Monomer Characterization: Despite their similarity in terms of di-substitution on PAH, key differences in terms of bond lengths, dihedral angles between phenol and acenaphthene/phenanthrene moieties were observed. For example, bond length between the oxygens pertaining to the phenols were 8.61 and 6.75Å for **M2** and M4, respectively. Such large distances between the oxygens (and therefore hydroxyl groups) is expected to facilitate intermolecular polymerization over intramolecular condensation between DFCH and **M2** or M4. This was further substantiated by the larger θ angle between the two phenolic groups present in **M2** (79°) compared to 56° in M4 (Figure 1). Conversely, in the crystal lattice planes, lower dihedral angles were observed between the phenol and acenaphthene (40°) in **M2** compared to phenol and phenanthrenes (65°) in M4. Interestingly, these values, in particular in M4, were substantially higher compared with linear bisphenols such as biphenol or bisphenol-A (36°).

FTIR analyses of monomers **M1**–**M2** (Figure S1) revealed several characteristic bands at ~3290, 1592 (also 1426 and 1368), 1265 (and 1100), corresponding to the presence of O-H vibration, C=C stretching vibration, C-O vibration (also C-H deformation vibration), respectively. Despite the significant overlap in the characteristic bands, presence of characteristic band in **M1** at 1694 cm-1 (C=O stretching vibration) provided evidence for the partial/complete retention of diketone in **M1**. Similarly, in **M3** and **M4** (Figure S1), several common characteristic bands were observed at 3500-

3100, 1589 (also 1504 and 1437), 1220, attributed to the broad O-H vibration, C=C stretching vibration, C-O stretching (also C–H vibration), respectively. Just like **M1**, characteristic band at 1663 cm-1 was observed in **M3** (and absent in **M4**) indicating the presence of characteristic C=O from the diketone (starting material).

These results were also in agreement with 13C-NMR experiments that showed presence of carbonyl signals at ~205 ppm in case of **M1** (Figure S4) and **M3** (Figure S10) that were absent in **M2** and **M4**. As both FTIR and 13C-NMR did not demonstrate mono-or di-substitution of ketones, 1H-NMR and 2D-NMR experiments were carried out to elucidate the chemical structures. 1H-NMR (in methanol-d6) of **M1** (Figure S2) showed six doublets (d) and two doublets of doublet (dd) signals at 8.22, 7.98, 7.90, 7.42, 6.7, and 7.0, and; 7.8, and 7.67, respectively. On the other hand, 1H-NMR of **M2** (Figure S6) showed three d and one dd signals at 7.78, 7.24, and 6.8; and, 7.56, respectively, with the differences between **M1** and **M2**, attributed to the differences in the symmetry (Cs vs C2v). Heteronuclear multiple bond correlation (HMBC) spectroscopic experiment (Figure S3) was used to fully assign the protons on **M1**. HMBC experiment showed the correlation between carbonyl group (205 ppm) on **M1** and the two protons (Ha and Hb at 7.98 and 7.8 ppm, respectively) present in the naphthalene moiety, indicating mono-substitution in the acenaphthoquinone. In addition, heteronuclear single quantum correlation spectroscopic (HSQC) experiment was carried out on **M1** (Figure S5) to partially assign the carbons, except the quaternary carbons present in **M1**. The differences in the chemical structures of **M3** and **M4** were similarly elucidated by 1H- and nuclear overhauser effect (NOESY)-NMR experiments. Like **M1**, 1H-NMR of **M3** (Figure S8) showed multiple d and dd signals, with these signals significantly decreasing in **M4** (Figure S11), due to the enhanced symmetry in **M4**. In addition, NOESY

experiments were carried out on **M3** and **M4** to fully assign the protons present in both **M3** and **M4** (Figures S9 and S14).

Crystal data for **M2**: $C_{24}H_{16}O_2$, the integration of the data based on a triclinic unit cell yielded a total of 11378 reflections to a maximum θ angle of 58.89° (0.90 Å resolution), of which 2323 were independent (average redundancy 4.898, completeness = 93.7%, Rint = 3.90%, Rsig = 3.64%) and 2084 (89.71%) were greater than 2σ (F2). The final cell constants of a = 9.0533(5) Å, b = 9.3686(5) Å, c = 10.9877(6) Å, α = 102.680(2) °, β = 106.275(2) °, γ = 93.165(3) °, volume = 865.97(8) Å3, are based upon the refinement of the XYZ-centroids of 305 reflections above 20 σ (I) with 8.636 < 2θ < 51.36°.

Crystal data for **M4**: $C_{28}H_{26}O_4$, the integration of the data based on a triclinic unit cell yielded a total of 75362 reflections to a maximum θ angle of 72.61° (0.81 Å resolution), of which 8842 were independent (average redundancy 8.523, completeness = 97.9%, Rint = 4.61%, Rsig = 2.95%) and 7699 (87.07%) were greater than 2σ (F2). Based on the refinement of the XYZ-centroids of 4031 reflections above 20 σ (I) with 7.117° < 2θ < 145.0°, final cell constants of a = 9.7233(4) Å, b = 10.5056(5) Å, c = 25.1367(11) Å, α = 85.381(2) °, β = 81.238(2) °, γ = 64.053(2) °, volume = 2281.64(18) Å3, were obtained.

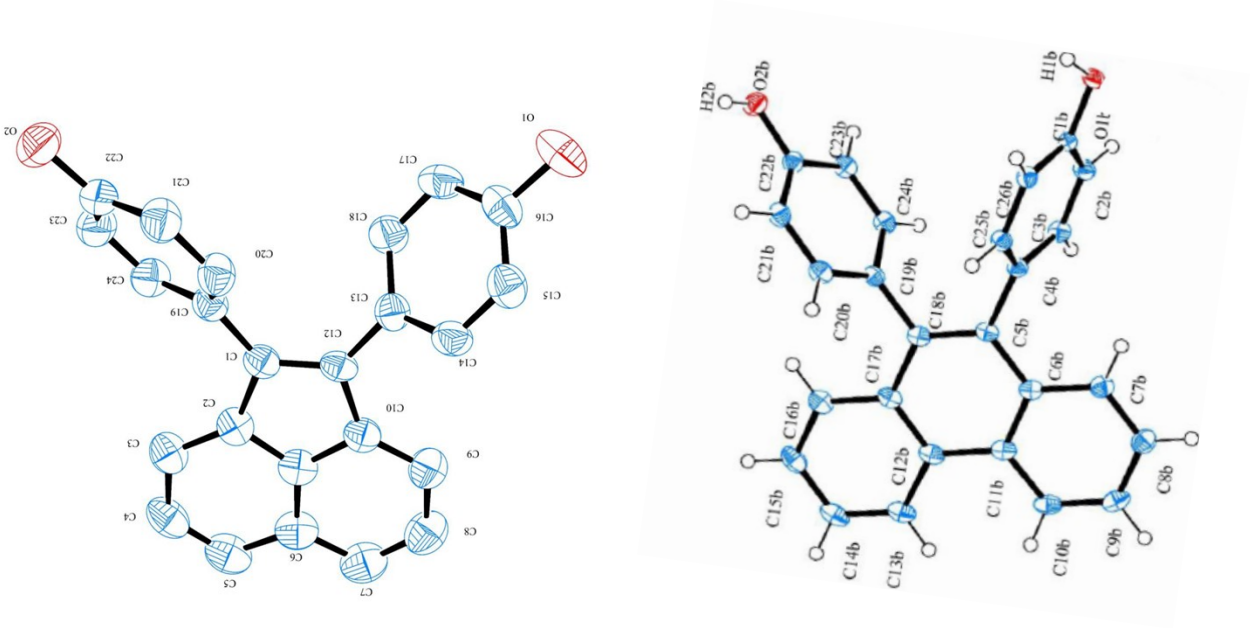

Figure A1. ORTEP representation of **M2** ($C_{24}H_{16}O_2$) and **M4** ($C_{28}H_{26}O_4$). This representation incorporates the atom labeling scheme for the independent non-hydrogen atoms. The thermal ellipsoids are scaled to enclose 50% probability.

Table 1. Bond lengths (Å) for **M2.**

O1-C16	1.387(5)	O1-H1	0.82
O2-C22	1.367(5)	O2-H2	0.82

C1-C12	1.376(5)	C1-C19	1.467(5)
C1-C2	1.485(5)	C2-C3	1.369(6)
C2-C11	1.409(6)	C3-C4	1.413(6)
C3-H3	0.93	C4-C5	1.363(7)
C4-H4	0.93	C5-C6	1.420(7)
C5-H5	0.93	C6-C11	1.385(6)
C6-C7	1.420(7)	C7-C8	1.366(7)
C7-H7	0.93	C8-C9	1.410(6)
C8-H8	0.93	C9-C10	1.372(6)
C9-H9	0.93	C10-C11	1.408(5)
C10-C12	1.475(5)	C12-C13	1.476(5)
C13-C18	1.386(6)	C13-C14	1.398(5)

C14-C15	1.377(6)	C14-H14	0.93
C15-C16	1.370(7)	C15-H15	0.93
C16-C17	1.389(6)	C17-C18	1.375(6)
C17-H17	0.93	C18-H18	0.93
C19-C20	1.393(6)	C19-C24	1.396(6)
C20-C21	1.377(6)	C20-H20	0.93
C21-C22	1.389(6)	C21-H21	0.93
C22-C23	1.372(6)	C23-C24	1.386(6)
C23-H23	0.93	C24-H24	0.93

Table 2. Bond angles (°) for **M2**.

C16-O1-H1	109.5	C22-O2-H2	109.5
C12-C1-C19	128.4(3)	C12-C1-C2	108.4(3)

C19-C1-C2	123.0(3)	C3-C2-C11	118.2(4)
C3-C2-C1	135.5(4)	C11-C2-C1	106.2(3)
C2-C3-C4	118.3(4)	C2-C3-H3	120.9
C4-C3-H3	120.9	C5-C4-C3	123.0(4)
C5-C4-H4	118.5	C3-C4-H4	118.5
C4-C5-C6	120.2(4)	C4-C5-H5	119.9
C6-C5-H5	119.9	C11-C6-C7	115.8(4)
C11-C6-C5	115.6(4)	C7-C6-C5	128.7(4)
C8-C7-C6	119.9(4)	C8-C7-H7	120.0
C6-C7-H7	120.0	C7-C8-C9	123.0(4)
C7-C8-H8	118.5	C9-C8-H8	118.5
C10-C9-C8	118.6(4)	C10-C9-H9	120.7
C8-C9-H9	120.7	C9-C10-C11	117.9(4)
C9-C10-C12	135.5(4)	C11-C10-C12	106.7(3)
C6-C11-C10	124.9(4)	C6-C11-C2	124.8(4)
C10-C11-C2	110.3(4)	C1-C12-C10	108.5(3)
C1-C12-C13	127.5(3)	C10-C12-C13	124.0(3)

C18-C13-C14	117.7(4)	C18-C13-C12	122.3(3)
C14-C13-C12	120.0(4)	C15-C14-C13	121.0(4)
C15-C14-H14	119.5	C13-C14-H14	119.5
C16-C15-C14	119.9(4)	C16-C15-H15	120.0
C14-C15-H15	120.0	C15-C16-O1	118.1(4)
C15-C16-C17	120.5(4)	O1-C16-C17	121.4(4)
C18-C17-C16	119.1(4)	C18-C17-H17	120.5
C16-C17-H17	120.5	C17-C18-C13	121.8(4)
C17-C18-H18	119.1	C13-C18-H18	119.1
C20-C19-C24	117.0(4)	C20-C19-C1	122.0(3)
C24-C19-C1	121.0(3)	C21-C20-C19	121.9(4)
C21-C20-H20	119.1	C19-C20-H20	119.1
C20-C21-C22	119.8(4)	C20-C21-H21	120.1
C22-C21-H21	120.1	O2-C22-C23	117.6(4)
O2-C22-C21	122.8(4)	C23-C22-C21	119.7(4)
C22-C23-C24	120.1(4)	C22-C23-H23	119.9
C24-C23-H23	119.9	C23-C24-C19	121.5(4)

C23-C24-H24	119.3	C19-C24-H24	119.3

Table 3. Bond lengths (Å) for **M4**.

O1A-C1A	1.3724(16)	O1A-H1A	0.8401
O2A-C22A	1.3759(15)	O2A-H2A	0.84
C1A-C2A	1.388(2)	C1A-C26A	1.3899(19)
C2A-C3A	1.381(2)	C2A-H2A1	0.95
C3A-C4A	1.3961(19)	C3A-H3A	0.95
C4A-C25A	1.3920(19)	C4A-C5A	1.4930(18)
C5A-C18A	1.3646(19)	C5A-C6A	1.4529(18)
C6A-C7A	1.410(2)	C6A-C11A	1.418(2)
C7A-C8A	1.374(2)	C7A-H7A	0.95
C8A-C9A	1.394(2)	C8A-H8A	0.95
C9A-C10A	1.370(2)	C9A-H9A	0.95
C10A-C11A	1.4163(19)	C10A-H10A	0.95
C11A-C12A	1.449(2)	C12A-C13A	1.415(2)
C12A-C17A	1.4194(19)	C13A-C14A	1.365(2)
C13A-H13A	0.95	C14A-C15A	1.401(2)
C14A-H14A	0.95	C15A-C16A	1.373(2)
C15A-H15A	0.95	C16A-C17A	1.412(2)
C16A-H16A	0.95	C17A-C18A	1.4525(18)
C18A-C19A	1.4968(18)	C19A-C24A	1.3921(18)
C19A-C20A	1.3979(18)	C20A-C21A	1.3858(19)
C20A-H20A	0.95	C21A-C22A	1.3872(18)

C21A-H21A	0.95	C22A-C23A	1.3860(18)
C23A-C24A	1.3892(18)	C23A-H23A	0.95
C24A-H24A	0.95	C25A-C26A	1.3848(19)
C25A-H25A	0.95	C26A-H26A	0.95
O1B-C1B	1.3790(15)	O1B-H1B	0.87(2)
O2B-C22B	1.3758(16)	O2B-H2B	0.90(2)
C1B-C26B	1.3861(18)	C1B-C2B	1.3871(18)
C2B-C3B	1.3872(18)	C2B-H2B1	0.95
C3B-C4B	1.3957(18)	C3B-H3B	0.95
C4B-C25B	1.3911(17)	C4B-C5B	1.4964(17)
C5B-C18B	1.3660(19)	C5B-C6B	1.4498(18)
C6B-C11B	1.4162(18)	C6B-C7B	1.4172(19)
C7B-C8B	1.373(2)	C7B-H7B	0.95
C8B-C9B	1.401(2)	C8B-H8B	0.95
C9B-C10B	1.367(2)	C9B-H9B	0.95
C10B-C11B	1.4155(19)	C10B-H10B	0.95
C11B-C12B	1.452(2)	C12B-C13B	1.4156(19)
C12B-C17B	1.4213(19)	C13B-C14B	1.372(2)
C13B-H13B	0.95	C14B-C15B	1.395(2)
C14B-H14B	0.95	C15B-C16B	1.377(2)
C15B-H15B	0.95	C16B-C17B	1.411(2)
C16B-H16B	0.95	C17B-C18B	1.4539(18)
C18B-C19B	1.4964(18)	C19B-C24B	1.3914(18)
C19B-C20B	1.3962(18)	C20B-C21B	1.3870(19)
C20B-H20B	0.95	C21B-C22B	1.3847(19)
C21B-H21B	0.95	C22B-C23B	1.3899(18)
C23B-C24B	1.3839(19)	C23B-H23B	0.95
C24B-H24B	0.95	C25B-C26B	1.3896(18)

C25B-H25B	0.95	C26B-H26B	0.95
O1S-C1S	1.4181(19)	O1S-H1S	0.85(2)
C1S-H1S1	0.98	C1S-H1S2	0.98
C1S-H1S3	0.98	O2S-C2S	1.406(2)
O2S-H2S	0.83(2)	C2S-H2S1	0.98
C2S-H2S2	0.98	C2S-H2S3	0.98
O3S-C3S	1.4142(19)	O3S-H3S	0.89(2)
C3S-H3S1	0.98	C3S-H3S2	0.98
C3S-H3S3	0.98	O4S-C4S	1.4300(19)
O4S-H4S	0.85(2)	C4S-H4S1	0.98
C4S-H4S2	0.98	C4S-H4S3	0.98

Table 4. Bond angles (°) for **M4**.

C1A-O1A-H1A	109.5	C22A-O2A-H2A	109.5
O1A-C1A-C2A	118.38(12)	O1A-C1A-C26A	121.59(13)
C2A-C1A-C26A	120.03(13)	C3A-C2A-C1A	119.56(12)
C3A-C2A-H2A1	120.2	C1A-C2A-H2A1	120.2
C2A-C3A-C4A	121.52(13)	C2A-C3A-H3A	119.2
C4A-C3A-H3A	119.2	C25A-C4A-C3A	117.91(12)
C25A-C4A-C5A	120.67(12)	C3A-C4A-C5A	121.42(12)
C18A-C5A-C6A	120.61(12)	C18A-C5A-C4A	120.61(12)
C6A-C5A-C4A	118.75(12)	C7A-C6A-C11A	118.94(13)
C7A-C6A-C5A	121.24(13)	C11A-C6A-C5A	119.81(13)
C8A-C7A-C6A	121.47(15)	C8A-C7A-H7A	119.3
C6A-C7A-H7A	119.3	C7A-C8A-C9A	119.68(15)

C7A-C8A-H8A	120.2	C9A-C8A-H8A	120.2
C10A-C9A-C8A	120.30(14)	C10A-C9A-H9A	119.8
C8A-C9A-H9A	119.8	C9A-C10A-C11A	121.58(15)
C9A-C10A-H10A	119.2	C11A-C10A-H10A	119.2
C10A-C11A-C6A	118.00(14)	C10A-C11A-C12A	122.44(13)
C6A-C11A-C12A	119.55(12)	C13A-C12A-C17A	117.84(13)
C13A-C12A-C11A	122.69(13)	C17A-C12A-C11A	119.46(12)
C14A-C13A-C12A	121.88(14)	C14A-C13A-H13A	119.1
C12A-C13A-H13A	119.1	C13A-C14A-C15A	120.22(14)
C13A-C14A-H14A	119.9	C15A-C14A-H14A	119.9
C16A-C15A-C14A	119.58(14)	C16A-C15A-H15A	120.2
C14A-C15A-H15A	120.2	C15A-C16A-C17A	121.45(14)
C15A-C16A-H16A	119.3	C17A-C16A-H16A	119.3
C16A-C17A-C12A	119.03(12)	C16A-C17A-C18A	121.19(12)
C12A-C17A-C18A	119.78(12)	C5A-C18A-C17A	120.75(12)
C5A-C18A-C19A	120.21(12)	C17A-C18A-C19A	119.02(12)
C24A-C19A-C20A	118.28(12)	C24A-C19A-C18A	120.59(11)
C20A-C19A-C18A	121.10(11)	C21A-C20A-C19A	121.25(12)
C21A-C20A-H20A	119.4	C19A-C20A-H20A	119.4
C20A-C21A-C22A	119.45(12)	C20A-C21A-H21A	120.3
C22A-C21A-H21A	120.3	O2A-C22A-C23A	117.32(11)
O2A-C22A-C21A	122.41(12)	C23A-C22A-C21A	120.27(12)
C22A-C23A-C24A	119.85(12)	C22A-C23A-H23A	120.1
C24A-C23A-H23A	120.1	C23A-C24A-C19A	120.86(12)
C23A-C24A-H24A	119.6	C19A-C24A-H24A	119.6
C26A-C25A-C4A	121.29(12)	C26A-C25A-H25A	119.4
C4A-C25A-H25A	119.4	C25A-C26A-C1A	119.68(13)
C25A-C26A-H26A	120.2	C1A-C26A-H26A	120.2

C1B-O1B-H1B	108.6(14)	C22B-O2B-H2B	111.7(14)
O1B-C1B-C26B	121.56(11)	O1B-C1B-C2B	117.95(11)
C26B-C1B-C2B	120.48(12)	C1B-C2B-C3B	119.26(12)
C1B-C2B-H2B1	120.4	C3B-C2B-H2B1	120.4
C2B-C3B-C4B	121.27(12)	C2B-C3B-H3B	119.4
C4B-C3B-H3B	119.4	C25B-C4B-C3B	118.41(12)
C25B-C4B-C5B	120.60(11)	C3B-C4B-C5B	120.95(11)
C18B-C5B-C6B	120.64(12)	C18B-C5B-C4B	120.22(12)
C6B-C5B-C4B	119.14(11)	C11B-C6B-C7B	118.92(12)
C11B-C6B-C5B	120.08(12)	C7B-C6B-C5B	120.99(12)
C8B-C7B-C6B	121.37(13)	C8B-C7B-H7B	119.3
C6B-C7B-H7B	119.3	C7B-C8B-C9B	119.61(14)
C7B-C8B-H8B	120.2	C9B-C8B-H8B	120.2
C10B-C9B-C8B	120.24(13)	C10B-C9B-H9B	119.9
C8B-C9B-H9B	119.9	C9B-C10B-C11B	121.76(13)
C9B-C10B-H10B	119.1	C11B-C10B-H10B	119.1
C10B-C11B-C6B	118.09(13)	C10B-C11B-C12B	122.49(12)
C6B-C11B-C12B	119.42(12)	C13B-C12B-C17B	118.19(13)
C13B-C12B-C11B	122.37(13)	C17B-C12B-C11B	119.44(12)
C14B-C13B-C12B	121.48(14)	C14B-C13B-H13B	119.3
C12B-C13B-H13B	119.3	C13B-C14B-C15B	120.29(13)
C13B-C14B-H14B	119.9	C15B-C14B-H14B	119.9
C16B-C15B-C14B	119.82(14)	C16B-C15B-H15B	120.1
C14B-C15B-H15B	120.1	C15B-C16B-C17B	121.32(14)
C15B-C16B-H16B	119.3	C17B-C16B-H16B	119.3
C16B-C17B-C12B	118.89(12)	C16B-C17B-C18B	121.36(13)
C12B-C17B-C18B	119.74(12)	C5B-C18B-C17B	120.66(12)
C5B-C18B-C19B	120.36(11)	C17B-C18B-C19B	118.92(12)

C24B-C19B-C20B	118.12(12)	C24B-C19B-C18B	120.46(11)
C20B-C19B-C18B	121.42(12)	C21B-C20B-C19B	121.14(12)
C21B-C20B-H20B	119.4	C19B-C20B-H20B	119.4
C22B-C21B-C20B	119.64(12)	C22B-C21B-H21B	120.2
C20B-C21B-H21B	120.2	O2B-C22B-C21B	122.34(12)
O2B-C22B-C23B	117.49(12)	C21B-C22B-C23B	120.17(12)
C24B-C23B-C22B	119.61(12)	C24B-C23B-H23B	120.2
C22B-C23B-H23B	120.2	C23B-C24B-C19B	121.31(12)
C23B-C24B-H24B	119.3	C19B-C24B-H24B	119.3
C26B-C25B-C4B	120.88(12)	C26B-C25B-H25B	119.6
C4B-C25B-H25B	119.6	C1B-C26B-C25B	119.66(11)
C1B-C26B-H26B	120.2	C25B-C26B-H26B	120.2
C1S-O1S-H1S	109.5(15)	O1S-C1S-H1S1	109.5
O1S-C1S-H1S2	109.5	H1S1-C1S-H1S2	109.5
O1S-C1S-H1S3	109.5	H1S1-C1S-H1S3	109.5
H1S2-C1S-H1S3	109.5	C2S-O2S-H2S	111.8(15)
O2S-C2S-H2S1	109.5	O2S-C2S-H2S2	109.5
H2S1-C2S-H2S2	109.5	O2S-C2S-H2S3	109.5
H2S1-C2S-H2S3	109.5	H2S2-C2S-H2S3	109.5
C3S-O3S-H3S	113.5(14)	O3S-C3S-H3S1	109.5
O3S-C3S-H3S2	109.5	H3S1-C3S-H3S2	109.5
O3S-C3S-H3S3	109.5	H3S1-C3S-H3S3	109.5
H3S2-C3S-H3S3	109.5	C4S-O4S-H4S	112.3(15)
O4S-C4S-H4S1	109.5	O4S-C4S-H4S2	109.5
H4S1-C4S-H4S2	109.5	O4S-C4S-H4S3	109.5
H4S1-C4S-H4S3	109.5	H4S2-C4S-H4S3	109.5

General procedure for synthesis of homopolymers **P1–P4**.

Homopolymers **P1–P4** were obtained following the representative procedure in which 2.00 g of **M1–M4** were added to a 20 mL scintillating vial. Followed by which, 1–3 mL of DMF, and 6 × of stoichiometric equivalent of trimethylamine were added. Finally, stoichiometric amounts of DFCH was added via syringe. The reaction mixture was stirred at rt for ~12 h and then reaction temperature was gradually adjusted to 40 °C (for ~6h) to 80 °C (for 74–86 h) before allowed to cool to rt. The reaction mixture was then precipice in 500 mL methanol: water mixture (50/50 vol/vol), and subsequently, Soxhlet extracted in methanol and hexane, respectively. The final product was dried in room temperature for 24 h and stored in a sealed container until further use.

Synthesis of homopolymer **P1**.

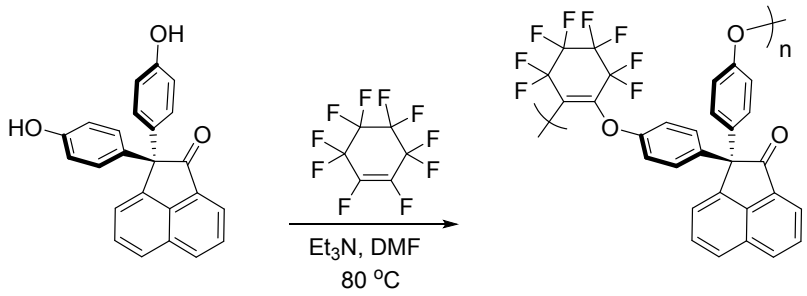

To a 20 mL scintillating vial equipped with magnetic stir bar was added 2.00 g (5.68 mmol) of **M1**, 3.45 g (34.1 mmol) of trimethylamine, and 2 mL of DMF. The reaction mixture was mildly stirred for 2 min, and then 1.49 g (5.68 mmol) of decafluorocyclohexene (DFCH) was added via syringe. The reaction mixture was stirred at rt for ~12 h and then

reaction temperature was gradually adjusted to 40 °C (for ~6h) to 80 °C (for 74–86 h) before allowed to cool to rt. The reaction mixture was then precipice in 500 mL methanol: water mixture (50/50 v/v), and subsequently, Soxhlet extracted in methanol and hexane, respectively, and dried under vacuum at 50 °C for 12h to give **P1 (**3.35 g, 74% yield) as white powder. IR: 1718, 1599, 1559, 1500, 1340, 1269, 1201, 1165, 1115, 997, 974, 818, 781, and 517 cm^{-1}; ^{1}H NMR ($CDCl_3$, 500 MHz) δ 8.26–7.99 (br), 7.99–7.84 (br), 7.84–7.56 (br), 7.56–7.26 (br), 7.25–6.93 (br), 6.93–6.71 (br), 6.71–6.57 (br), 6.45–6.15 (br); ^{19}F NMR ($CDCl_3$, 470 MHz,) δ –73.4 (0.23 F, s), –115.4 (4 F, s), –133.5 (4 F, s).

Synthesis of homopolymer **P2**.

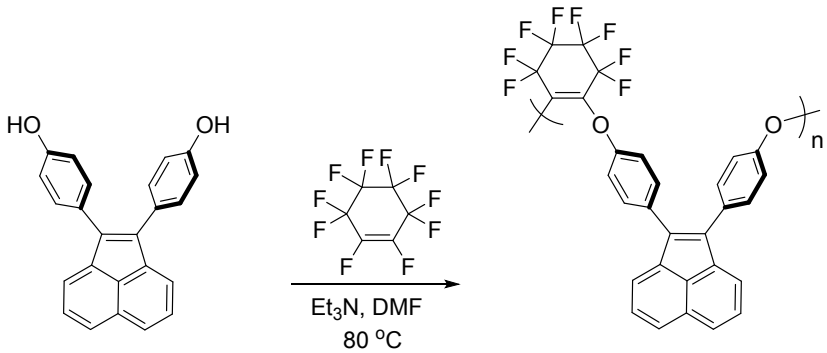

Homopolymer **P2** was synthesized using the same procedure as **P1** by using **M2** as monomer. After, dried under vacuo produced **P2 (**3.26 g, 70% yield) as white powder. IR: 3040, 2924, 1664, 1560, 1507, 1484, 1431, 1338, 1266, 1192, 1162, 1119, 995, 969, 820, 768, 686, 607, 549, and 522 cm^{-1}; ^{1}H NMR ($CDCl_3$, 500 MHz) δ 8.26–7.96 (br), 7.96–7.69

(br), 7.69–7.46 (br), 7.46–6.98 (br), 6.98–6.80 (br), 6.80–6.23; ^{19}F NMR ($CDCl_3$, 470 MHz,) δ –59.3 (0.11 F, s), –0.73 (0.19 F, s), –109.2 (0.29 F, s), –115.25 (4 F, m), –121.9 (0.43 F, s), –133.4 (4 F, s).

Synthesis of homopolymer **P3**.

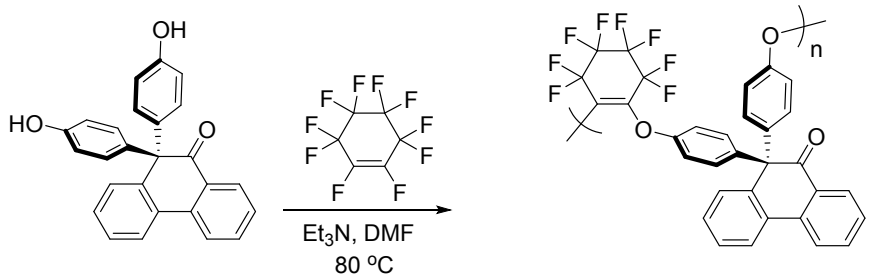

Homopolymer **P3** was synthesized using the same procedure as **P1** by using **M3** as monomer. After, dried under vacuo produced **P3 (**3.27 g, 77% yield) as white powder. IR: 1685, 1596, 1500, 1450, 1405, 1339, 1267, 1201, 1165, 1123, 998, 972, 819, 773, 733, 660, and 519 cm^{-1}; ^{1}H NMR ($CDCl_3$, 500 MHz) δ 8.09–7.79 (br), 7.79–7.55 (br), 7.55–7.28 (br), 7.24–6.95 (br), 6.95–6.65 (br), 6.65–6.34 (br), 6.34–5.85 (br); ^{19}F NMR ($CDCl_3$, 470 MHz,) δ –73.4 (0.13 F, s), –115.6 (4 F, s), –133.5 (4 F, s).

Synthesis of homopolymer **P4.**

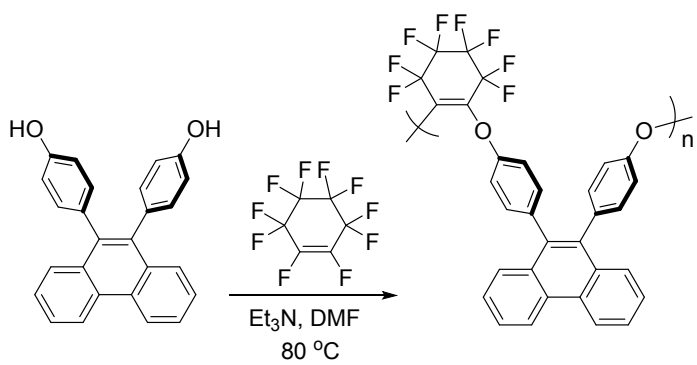

Homopolymer **P4** was synthesized using the same procedure as **P1** by using **M4** as monomer. After, dried under vacuo produced **P4 (**3.03 g, 68% yield) as white powder. IR: 3069, 1670, 1605, 1580, 1527, 1502, 1448, 1420, 1339, 1269, 1239, 1162, 1123, 1101, 997, 968, 887, 857, 809, 757, 725, 624, 570, 507, and 477 cm^{-1}; ^{1}H NMR ($CDCl_3$, 500 MHz) δ 8.87–8.60 (br), 7.73–7.27 (br), 7.19–6.78 (br), 6.65–6.30 (br); ^{19}F NMR ($CDCl_3$, 470 MHz,) δ –75.7 (0.02 F, s), –114.1 (0.39 F, s), –115.6 (4 F, s), –129.6, –133.4 (4 F, m), –151.3(0.04 F, s).

Synthesis of homopolymer **P5.**

Homopolymer **P5** was synthesized using the same procedure as **P1** by using bisphenol A as monomer. After, dried under vacuo produced **P5 (**2.6 g, 66% yield) as white powder. IR: 2968, 1663, 1603, 1502, 1341, 1271, 1199, 1165, 1123, 1015, 998, 974, 914, 827, 723, and 553 cm^{-1}; ^{1}H NMR ($CDCl_3$, 500 MHz) δ 7.24–6.8 (br), 6.8–6.65 (br), 6.54–6.37 (br); ^{19}F NMR ($CDCl_3$, 470 MHz,) δ –73.4 (0.67 F, s), –74.3 (0.30 F, s), –109.4 (0.8 F, s), –115.4 (4 F, s), –133.5 (4 F, s).

Synthesis of 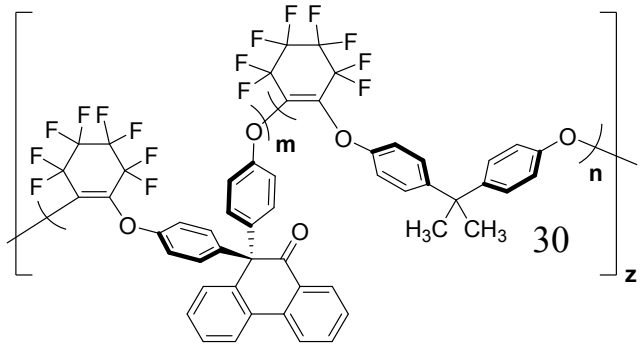 random copolymer **P6.**

m≠n

In a 20 mL vial equipped with magnetic stir bar was added 1.44 g (3.82 mmol) of **M3**, 0.87 g (3.82 mmol) of bisphenol A, 3.09 (30.53 mmol) of trimethylamine, and 2 mL of anhydrous DMF. The reaction mixture was mildly stirred for 2 min, and then 2.00 g (7.64 mmol) of decafluorocyclohexene (DFCH) was added via syringe. The reaction mixture was stirred at rt for ~12 h and then reaction temperature was gradually adjusted to 40 °C (for ~6h) to 80 °C (for 74–86 h) before allowed to cool to rt. The reaction mixture was then precipice in 500 mL methanol: water mixture (50/50 v/v), and subsequently, Soxhlet extracted in methanol and hexane, respectively, and dried under vacuum at 50 °C for 12h to give **P6 (**2.85 g, 71% yield) as white powder. IR: 1684, 1602, 1559, 1502, 1451, 1411, 1341, 1271, 1241, 1201, 1166, 1125, 993, 975, 829, 774, 735, 661, 525, and 481cm^{-1}; ^{19}F NMR ($CDCl_3$, 470 MHz,) δ –73.4 (0.32 F, s), –74.4 (0.1 F, s), –109.4(0.07 F, s), –115.4 (4 F, m), –133.5(4 F, s).

Synthesis of homopolymer **P7**

To a 20 mL scintillating vial equipped with magnetic stir bar was added 2.00 g (5.68 mmol) of **M1**, 3.45 g (34.1 mmol) of trimethylamine, and 2 mL of DMF. The reaction mixture was mildly stirred for 2 min, and then 1.49 g (5.68 mmol) of decafluorocyclohexene (DFCH) was added via syringe. The reaction mixture was stirred at rt for ~12 h and then reaction temperature was gradually adjusted to 120 °C (for ~6h) before allowed to cool to rt. The reaction mixture was then precipitated in 500 mL methanol: water mixture (50/50 v/v) to give **P7**.

Synthesis of homopolymer **P8**

Homopolymer **P8** was synthesized using the same procedure as **P7** by using **M3** as monomer.

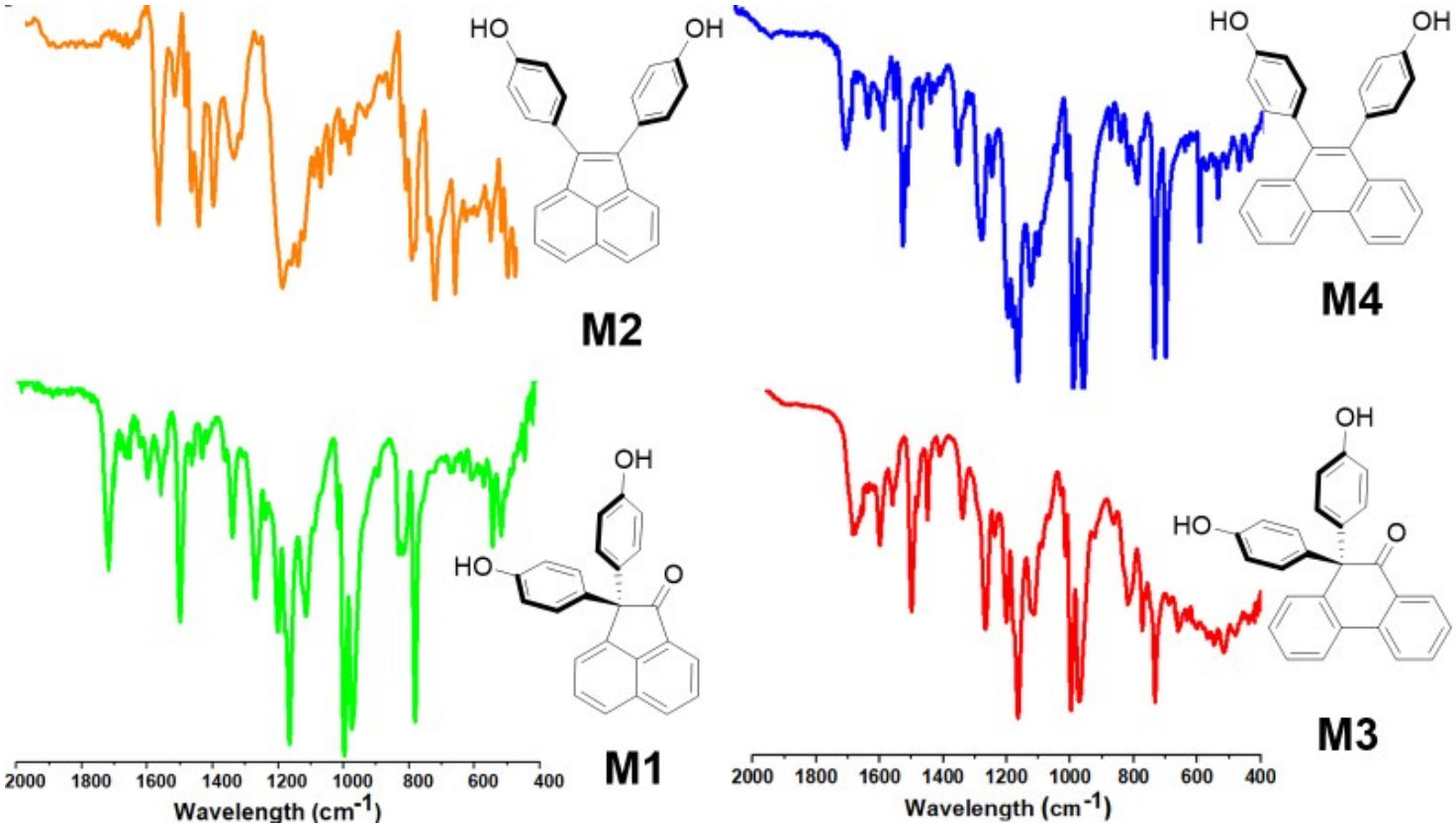

Figure S1. Fourier Transform Infrared (FT-IR) spectroscopic analyses of bisphenol **M1–M4**.

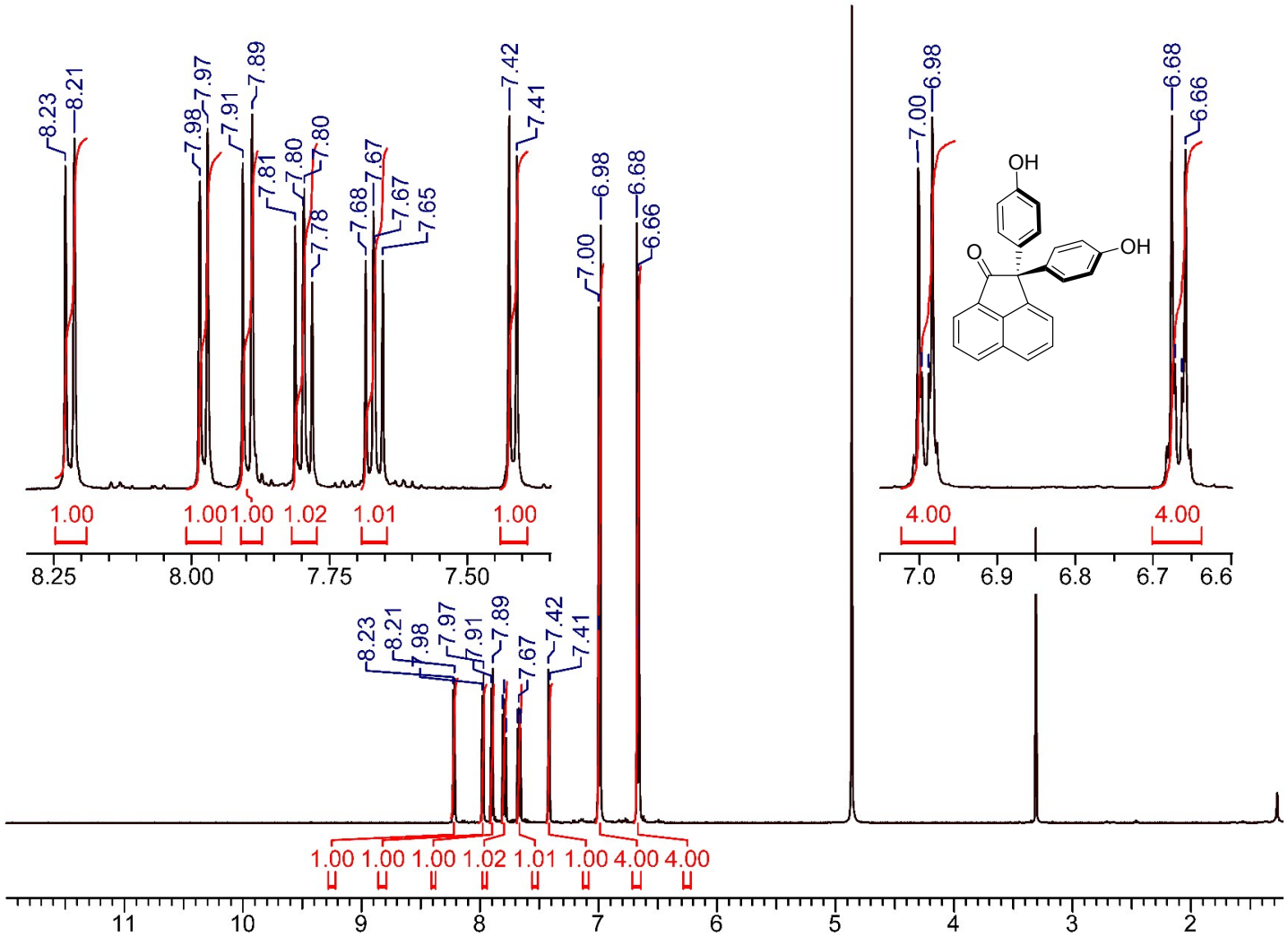

Figure S2. ^{1}H-NMR spectra of **M1** in CD_3OD.

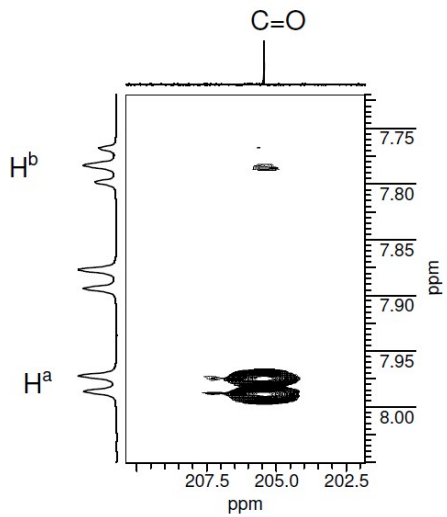

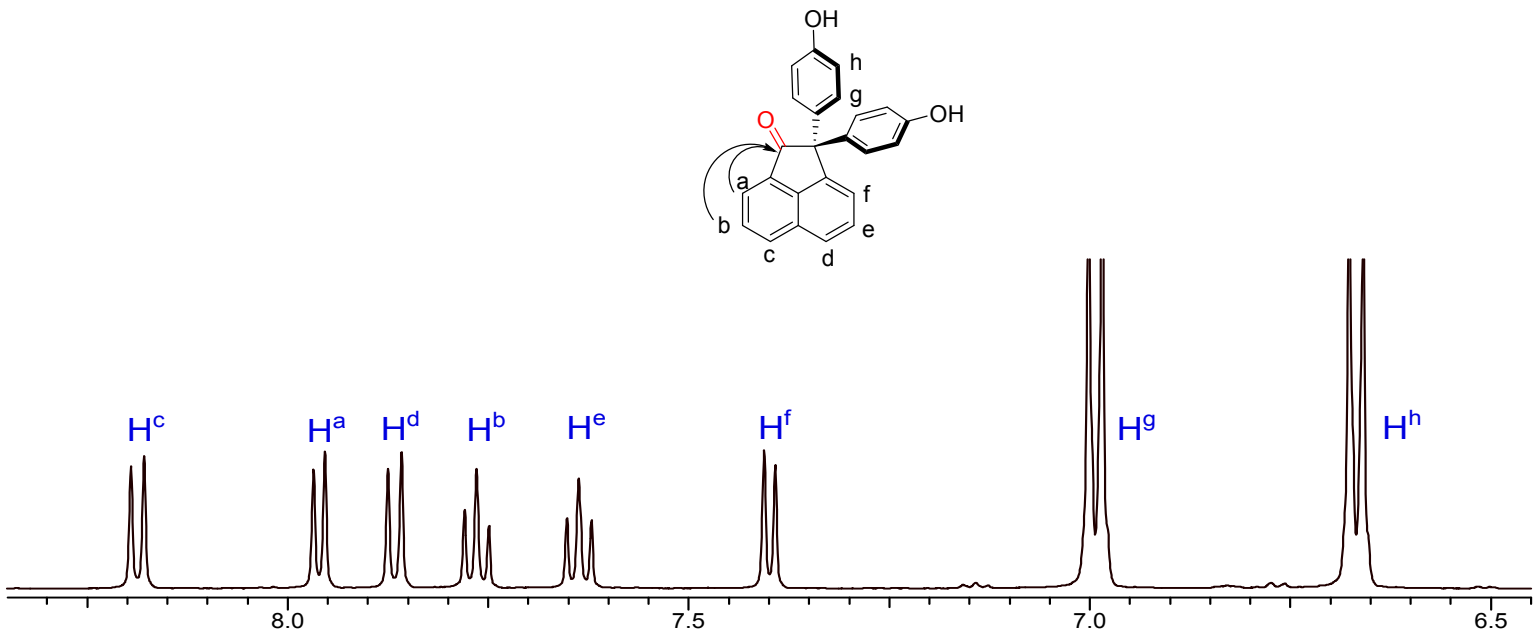

Figure S3. Heteronuclear multiple bond correlation (HMBC) spectroscopy and ^{1}H-NMR spectra of **M1** in CD_3OD.

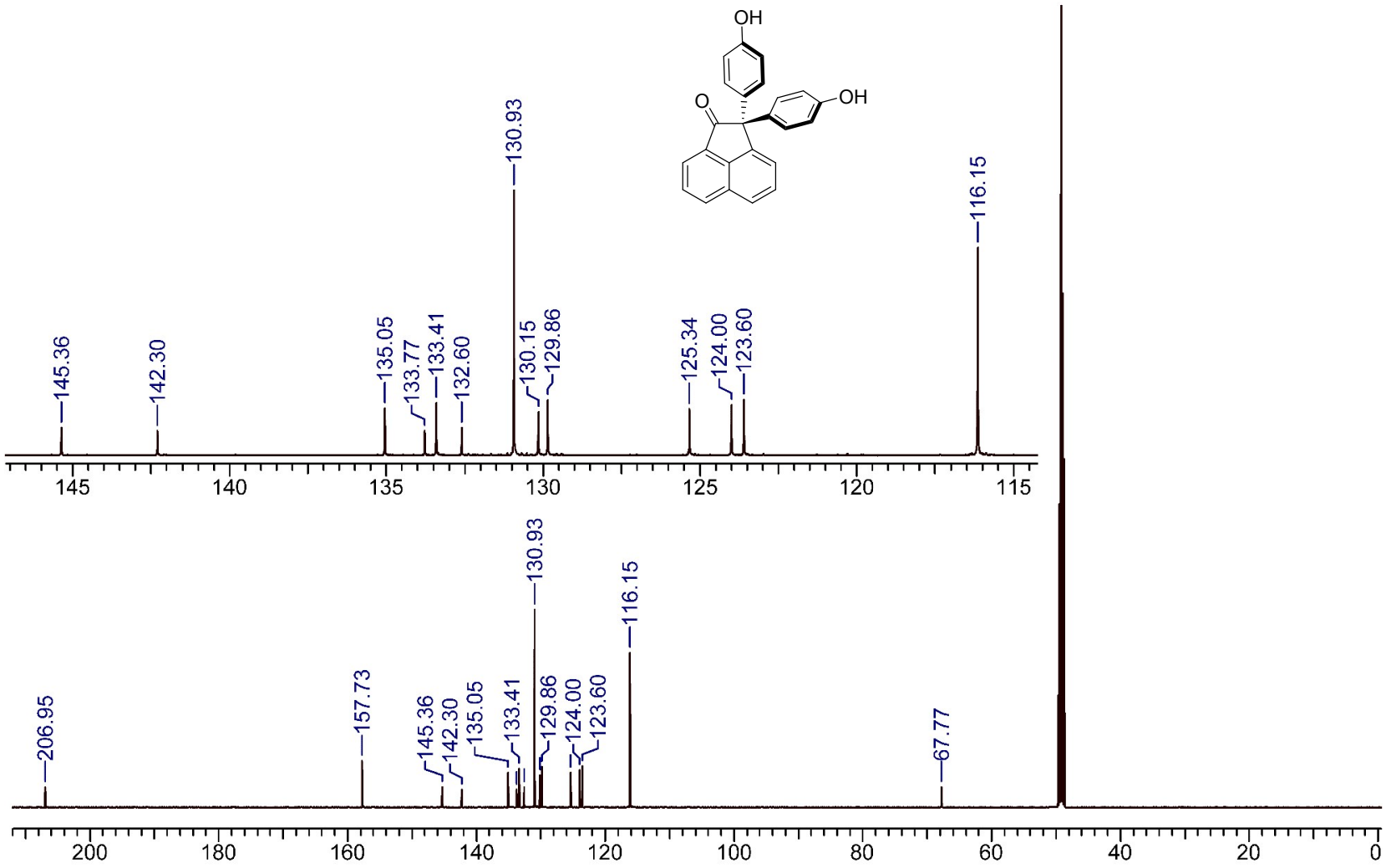

Figure S4. ^{13}C-NMR spectra of **M1** in CD_3OD.

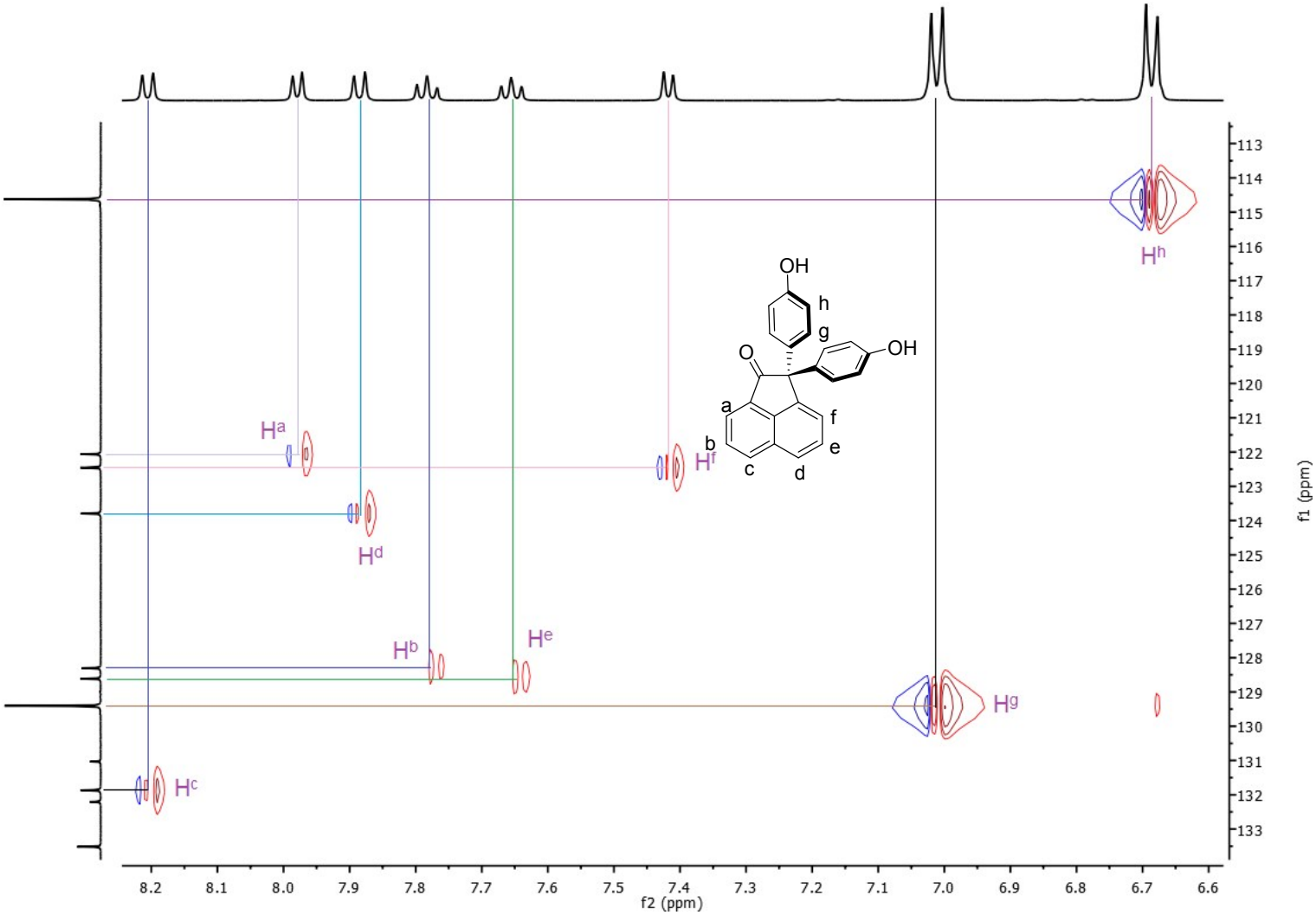

Figure S5. Heteronuclear single quantum coherence (HSQC) spectra of **M1** in CD_3OD.

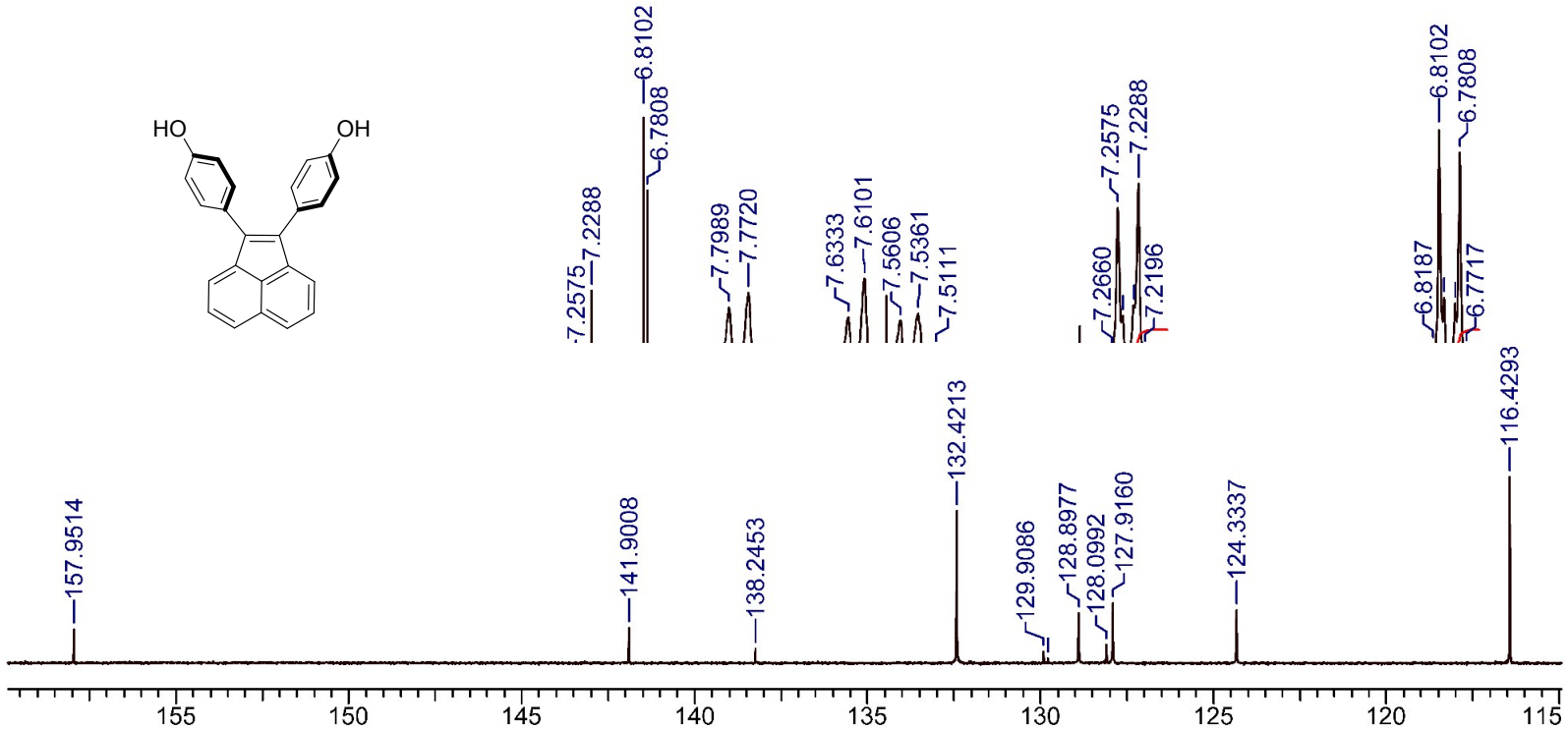

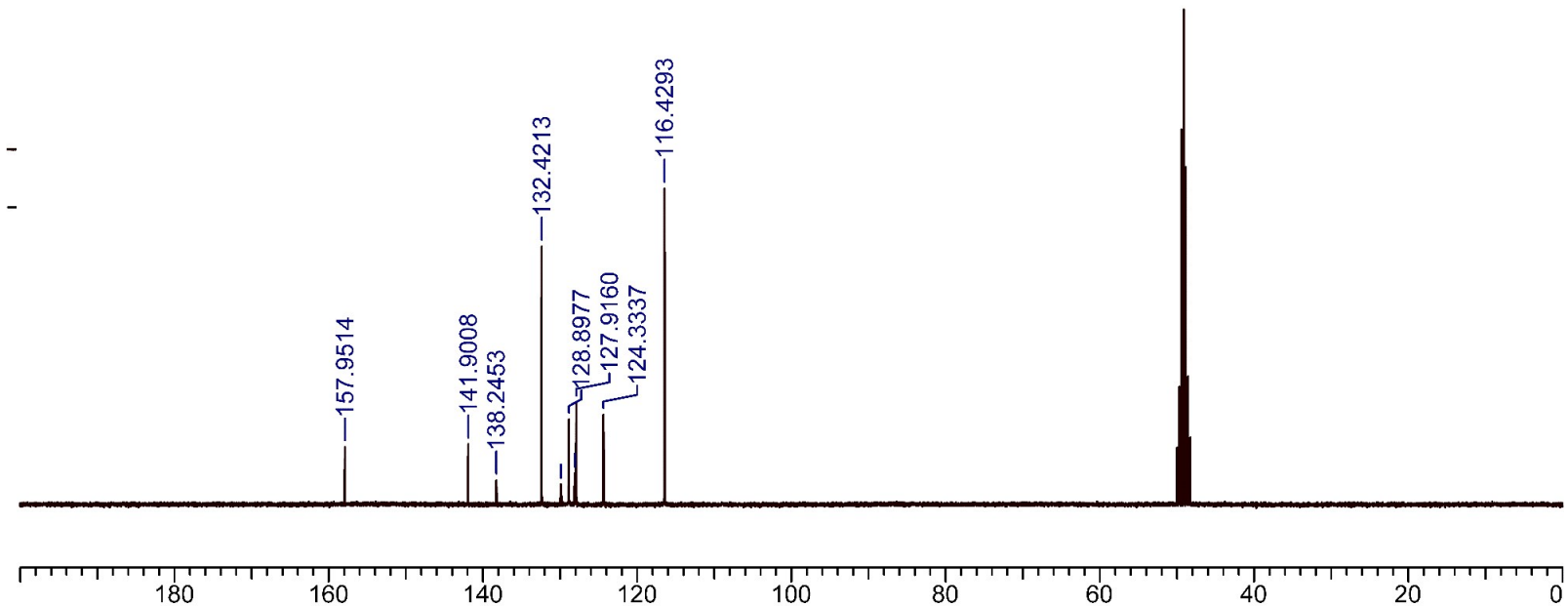

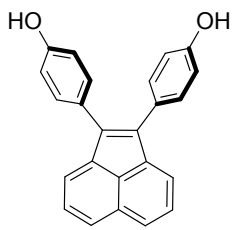

Figure S6. ^{1}H-NMR spectra of **M2** in CD_3OD.

Figure S7. ^{13}C-NMR spectra of **M2** in CD_3OD.

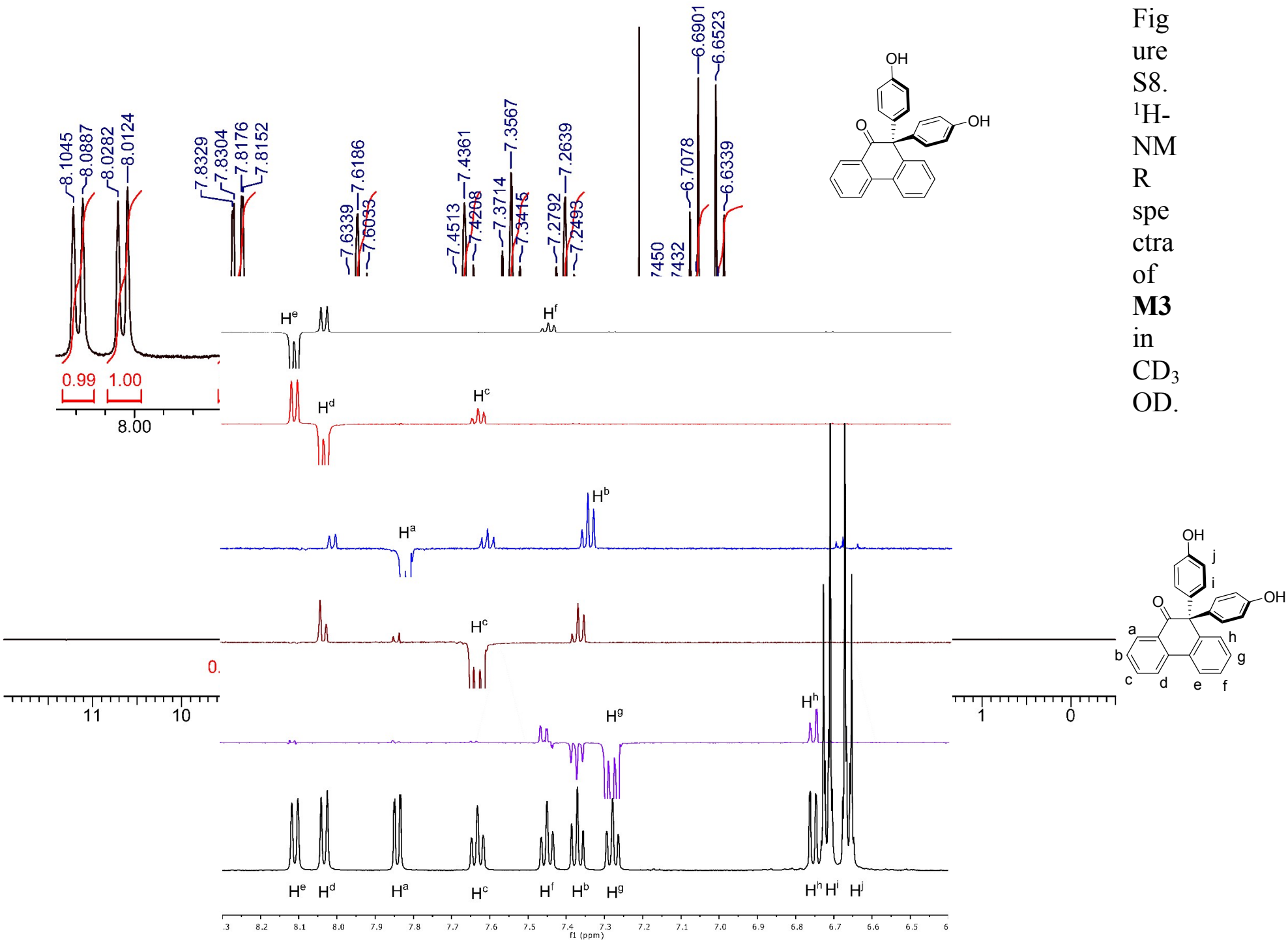

Figure S8. ^{1}H-NMR spectra of **M3** in CD_3OD.

Figure S9. NOESY spectra of **M3** in CD_3OD.

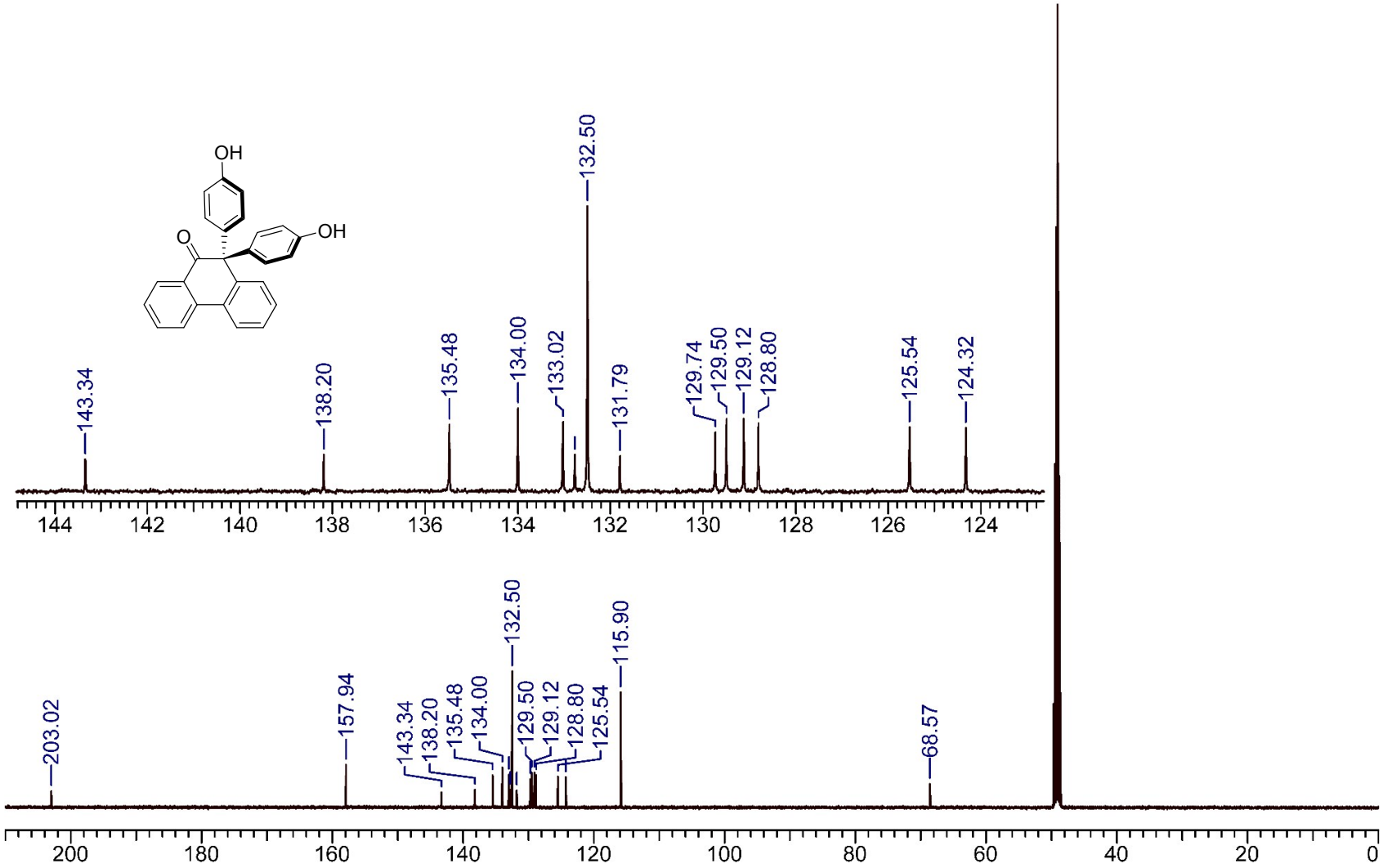

Figure S10. ^{13}C- NMR spectra of **M3** in CD_3OD.

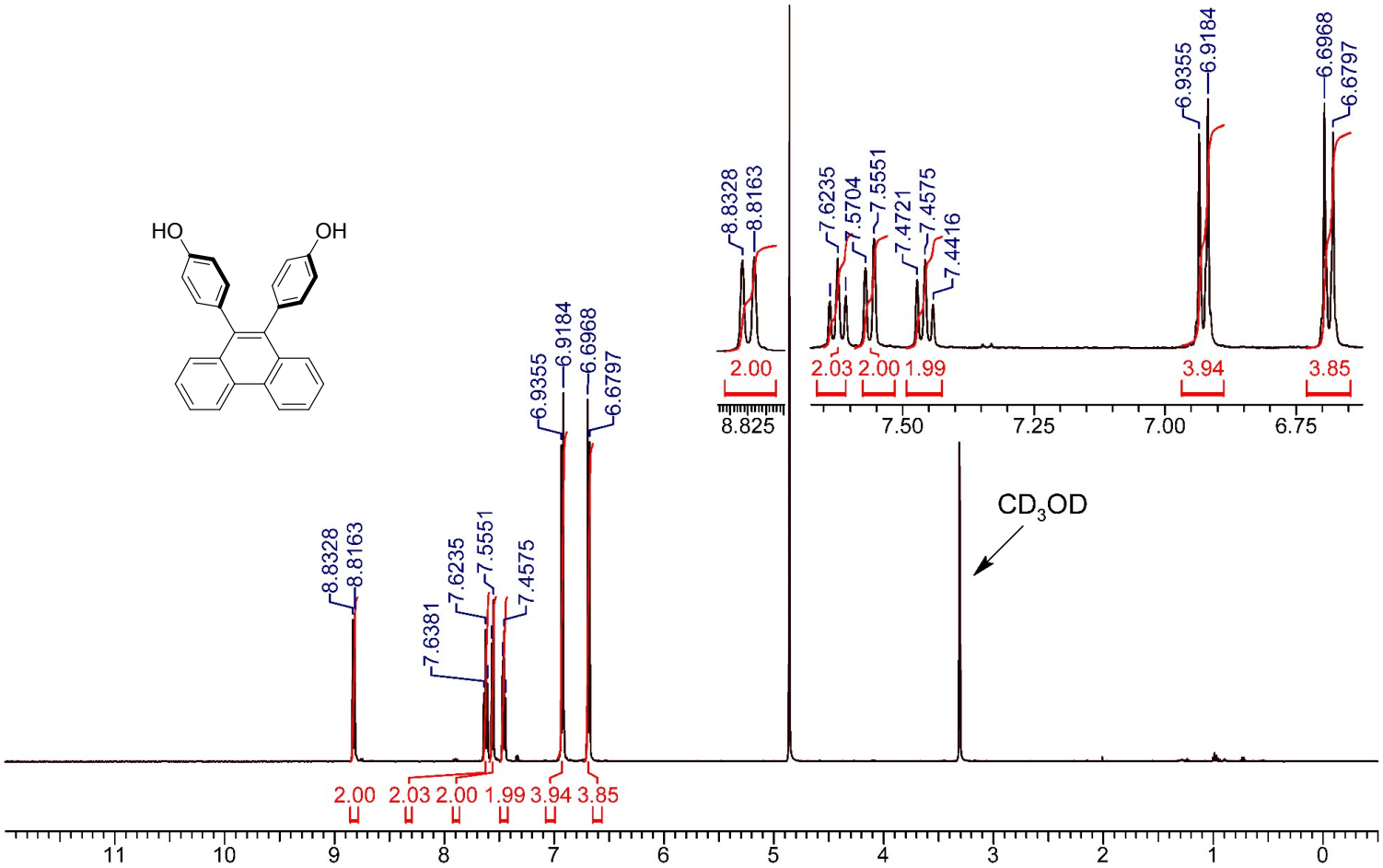

Figure S11. ^{1}H-NMR spectra of **M4** in CD_3OH.

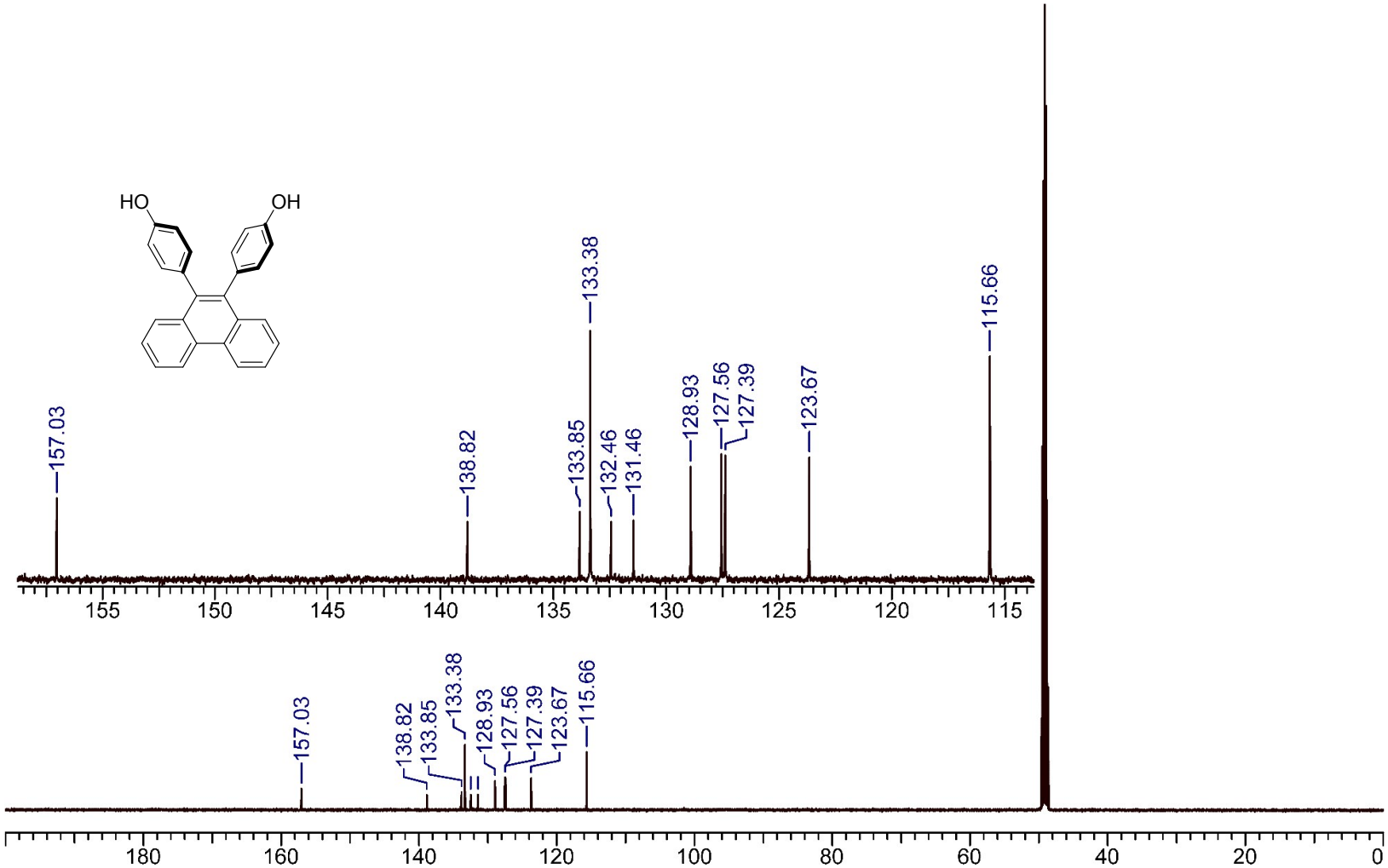

Figure S12. ^{13}C-NMR spectra of **M4** in CD_3OD.

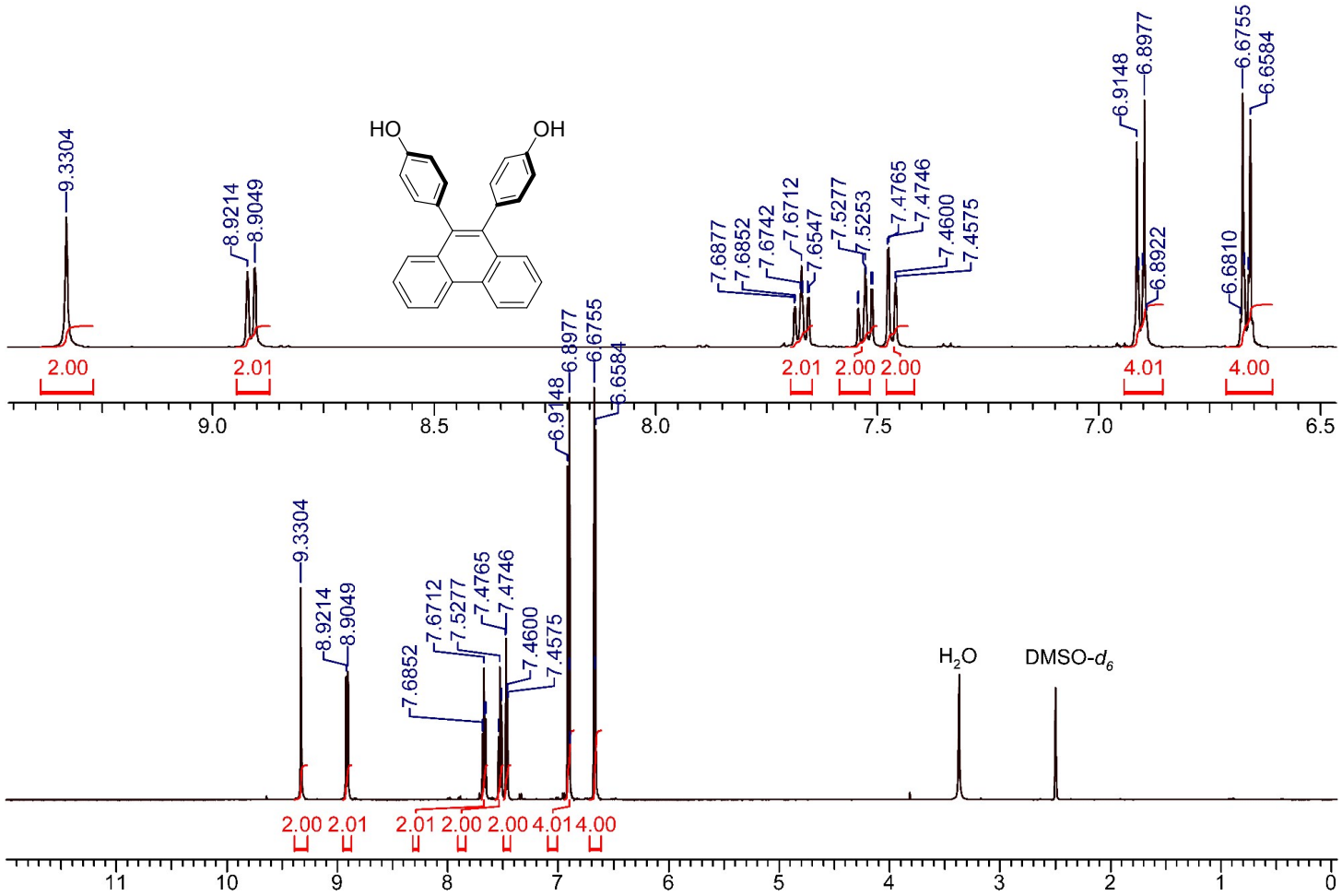

Figure S13. ^{1}H-NMR spectra of **M4** in DMSO-d_6.

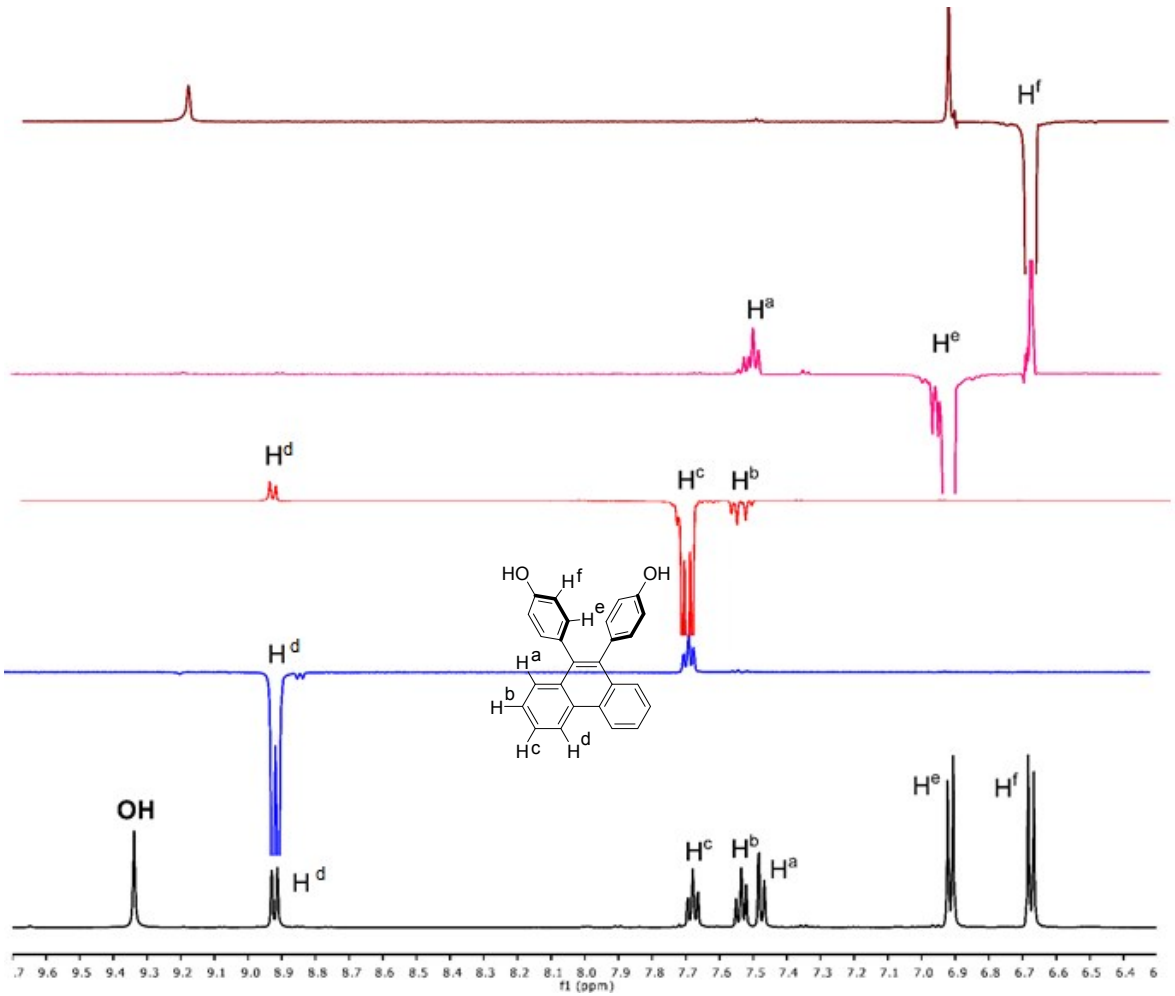

Figure S14.

NOESY NMR spectra of **M4** in DMSO-d_6.

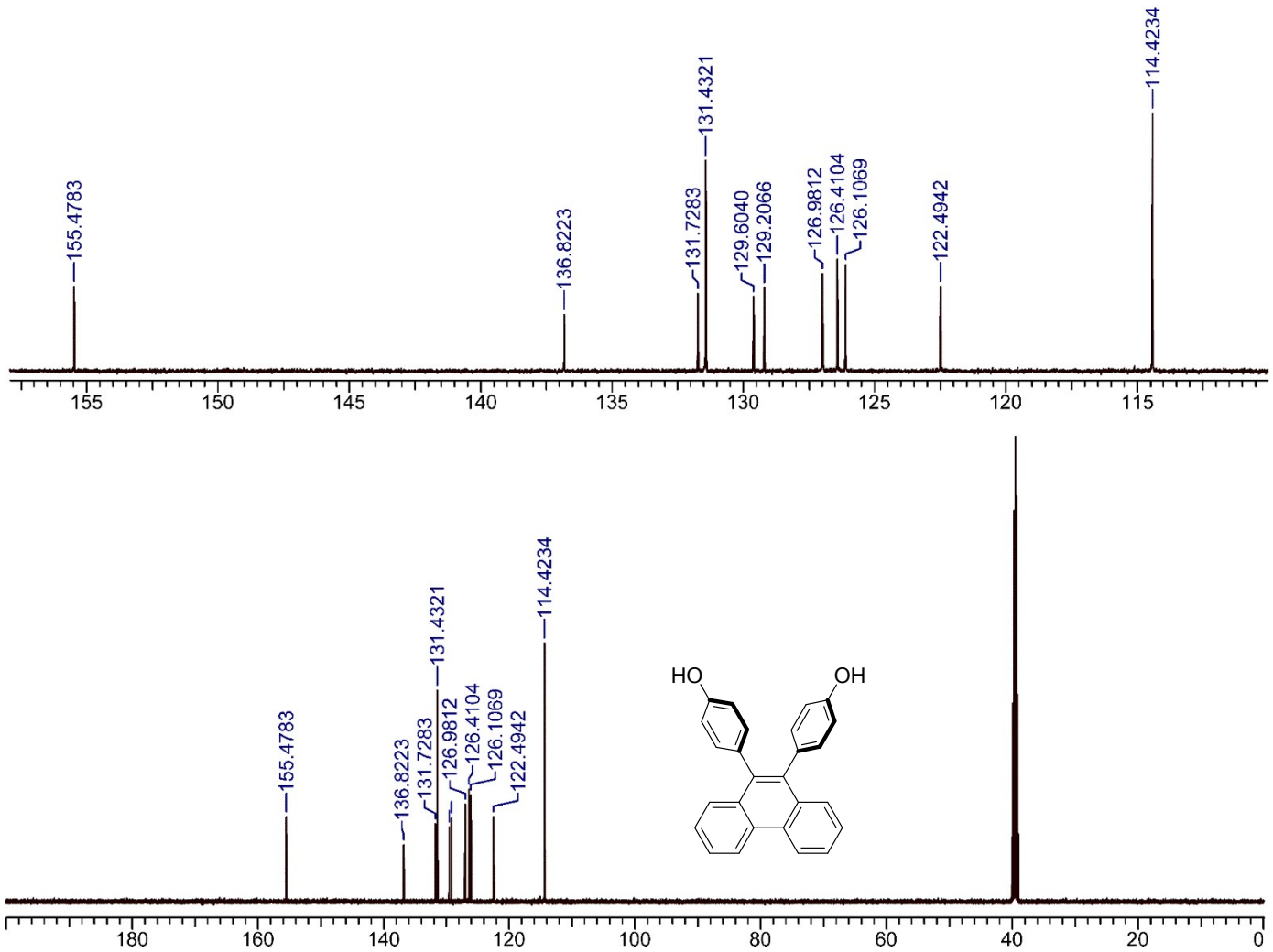

Figure S15. ^{13}C-NMR spectra of **M4** in CD_3OD.

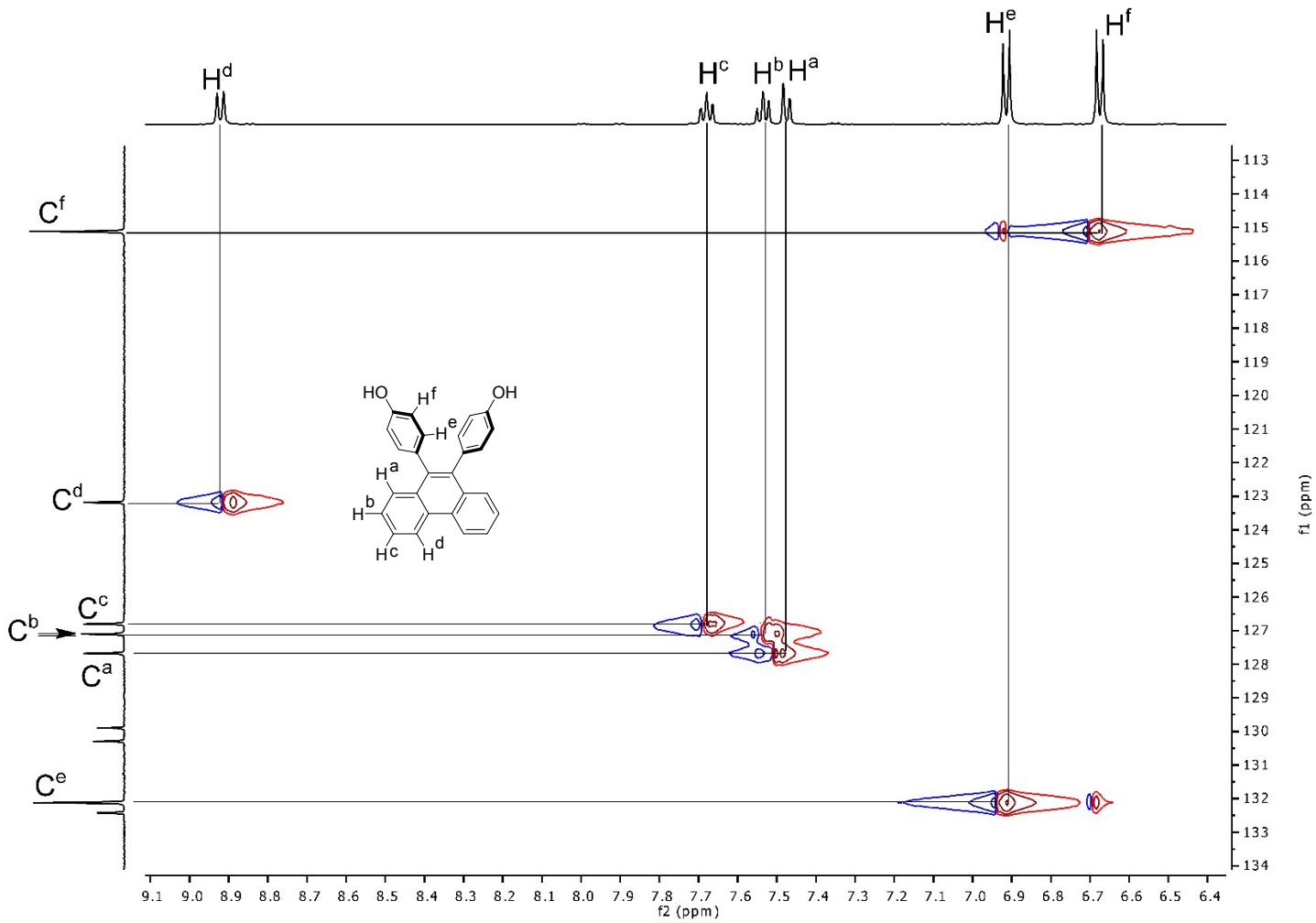

Figure S16. Heteronuclear single quantum coherence (HSQC) spectra of **M4** in DMSO-d_6.

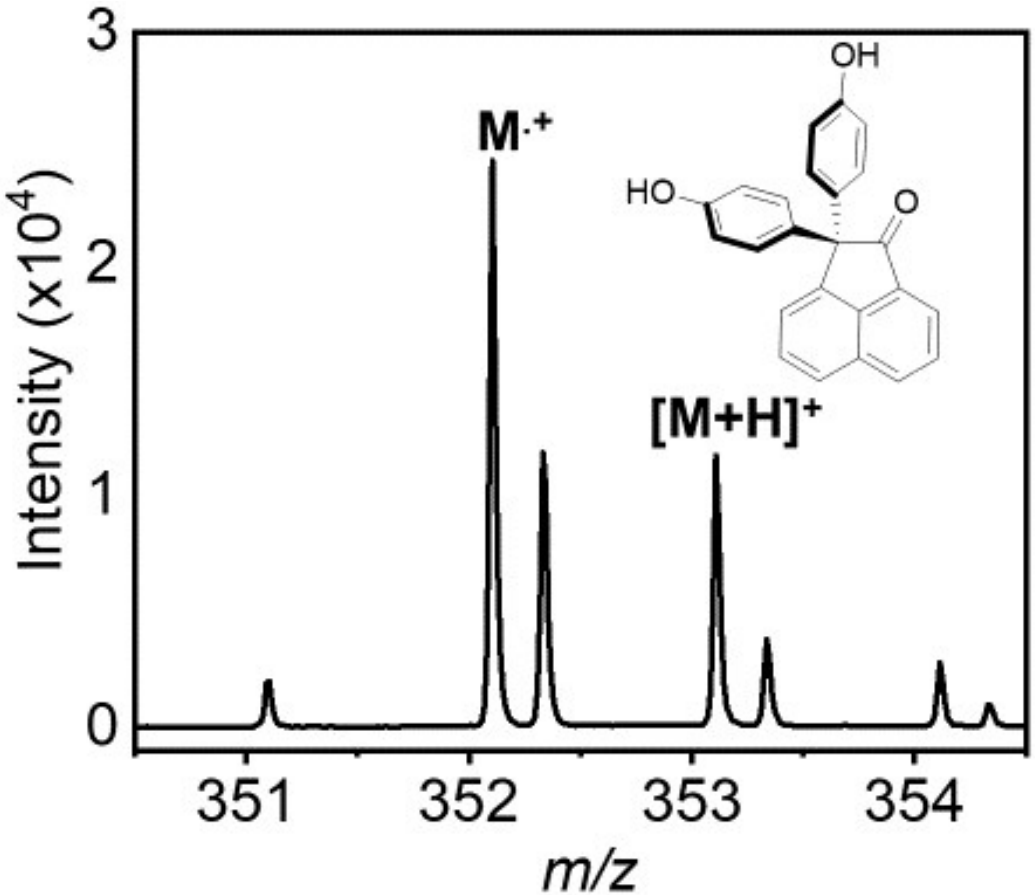

Figure S17. High resolution mass spectrometric analyses of **M1**.

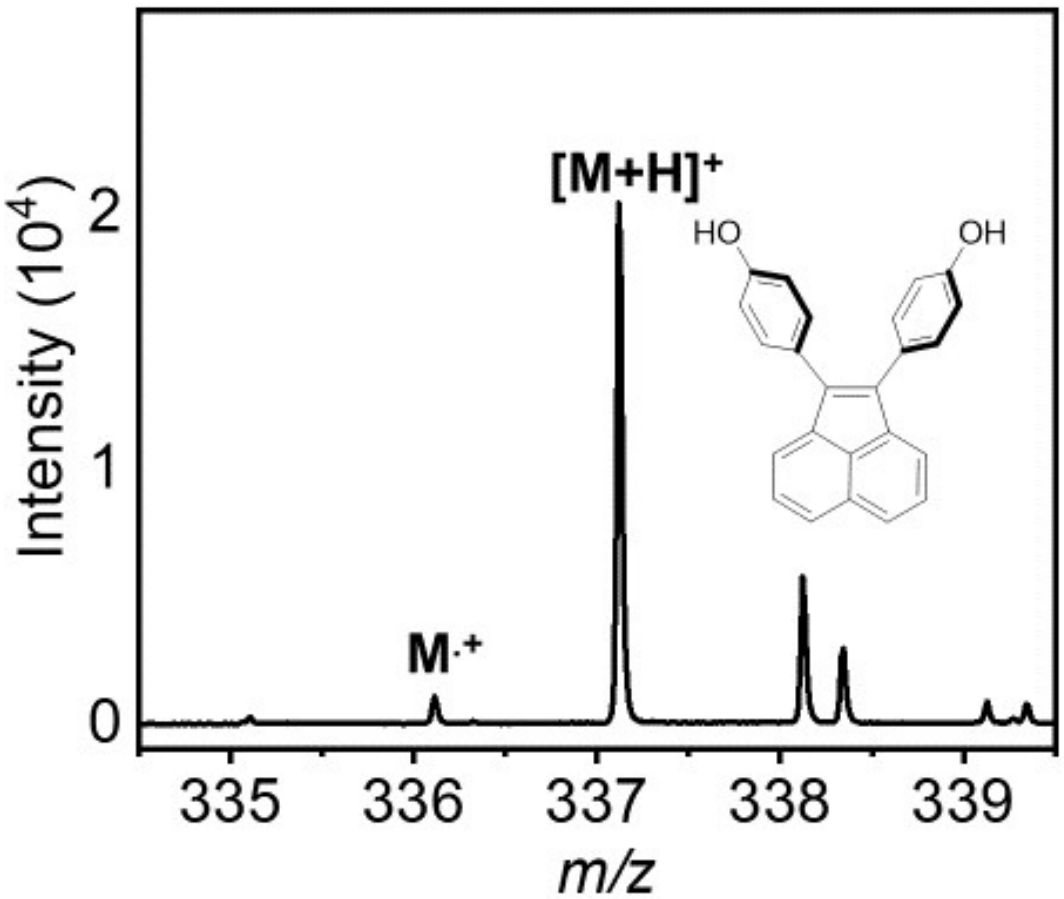

Figure S18. High resolution mass spectrometric analyses of **M2**.

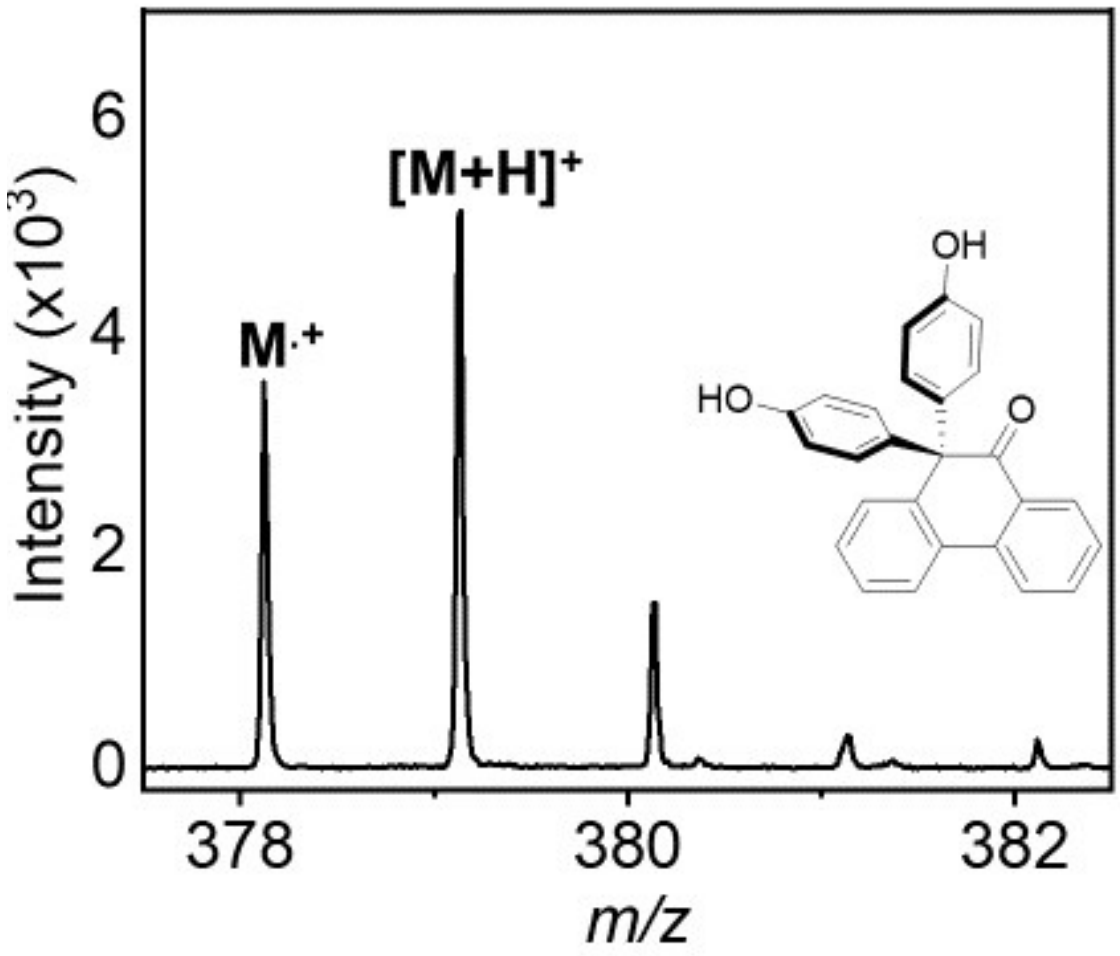

Figure S19. High resolution mass spectrometric analyses of **M3**.

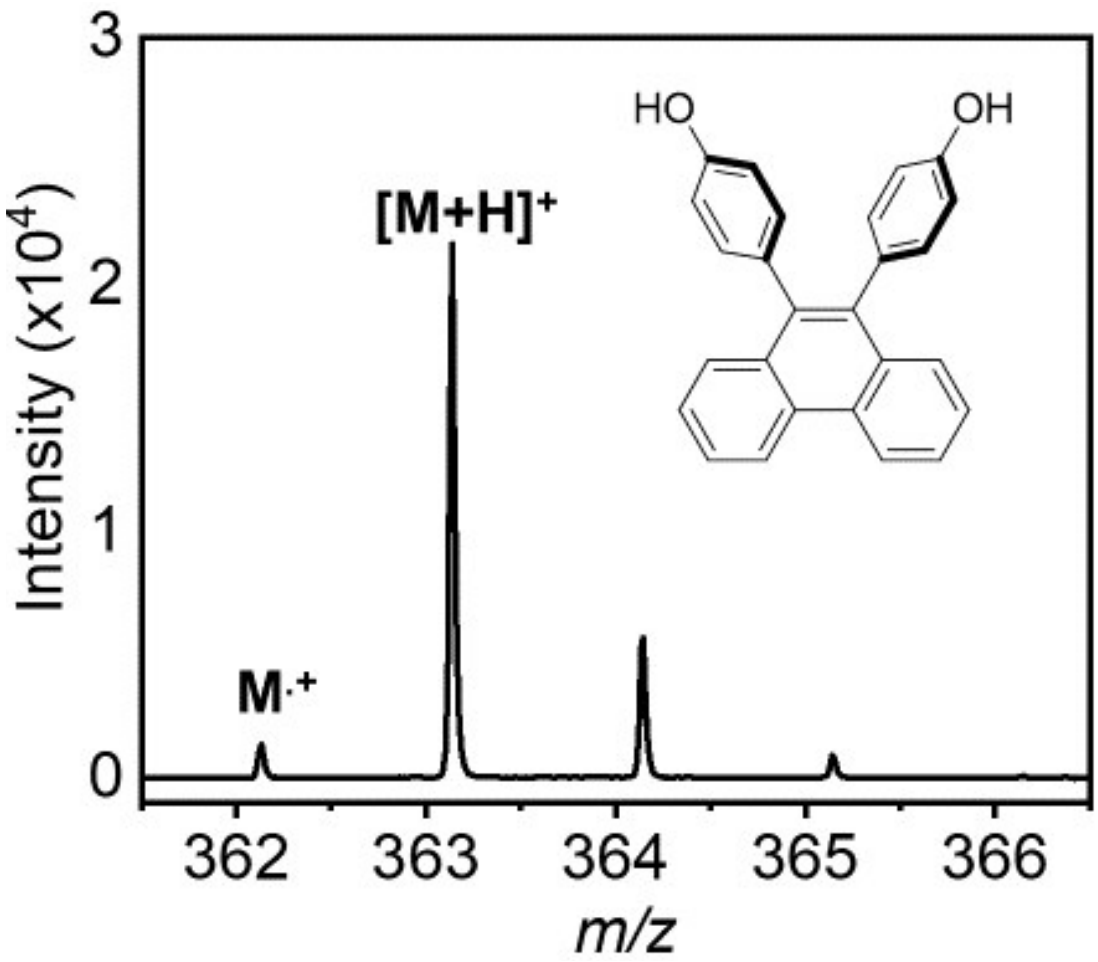

Figure S20. High resolution mass spectrometric analyses of **M4**.

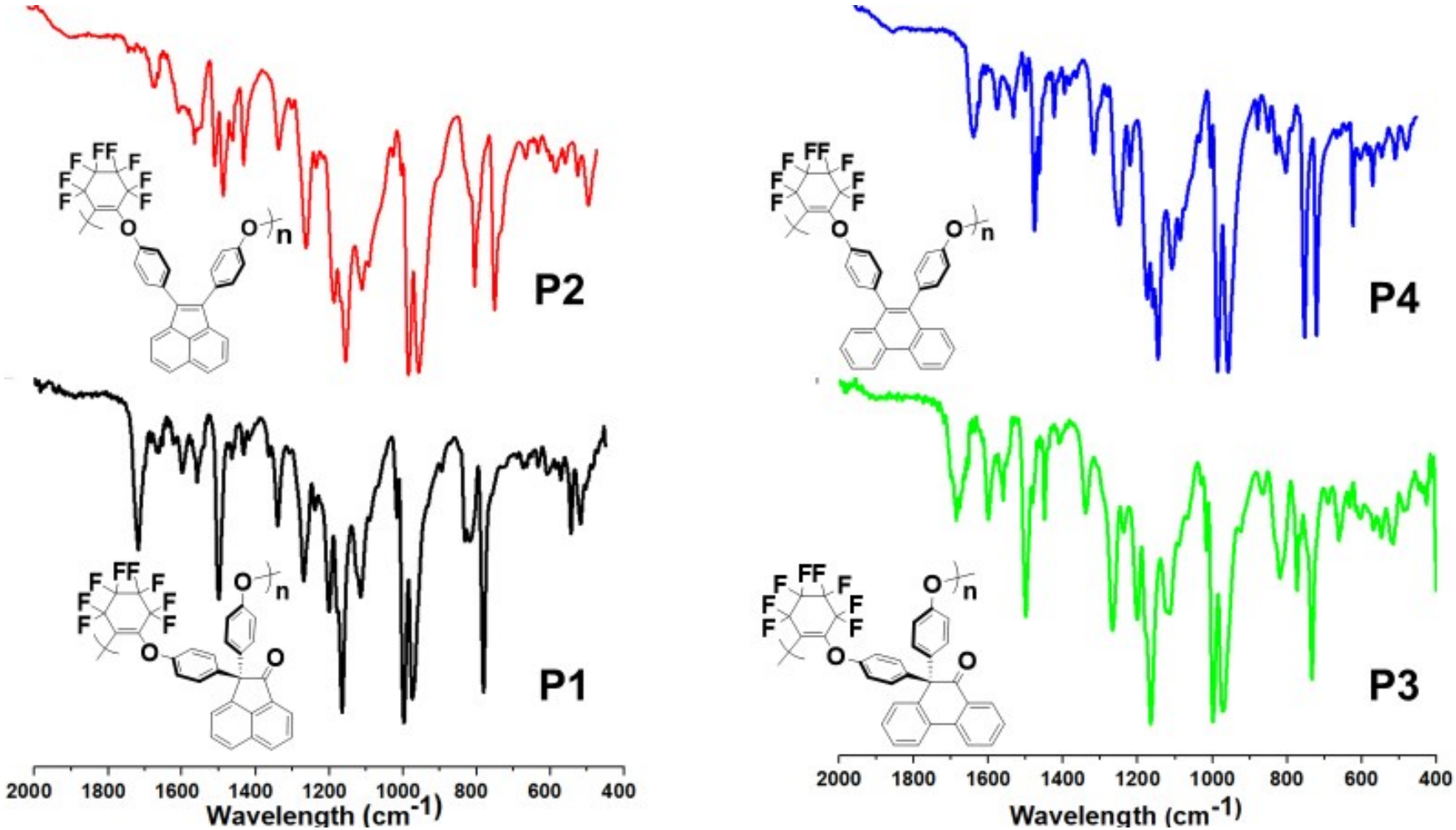

Figure S21. Fourier transform infrared analyses of **P1**–**P4** between the wavelengths 2000 and 400 cm^{-1}.

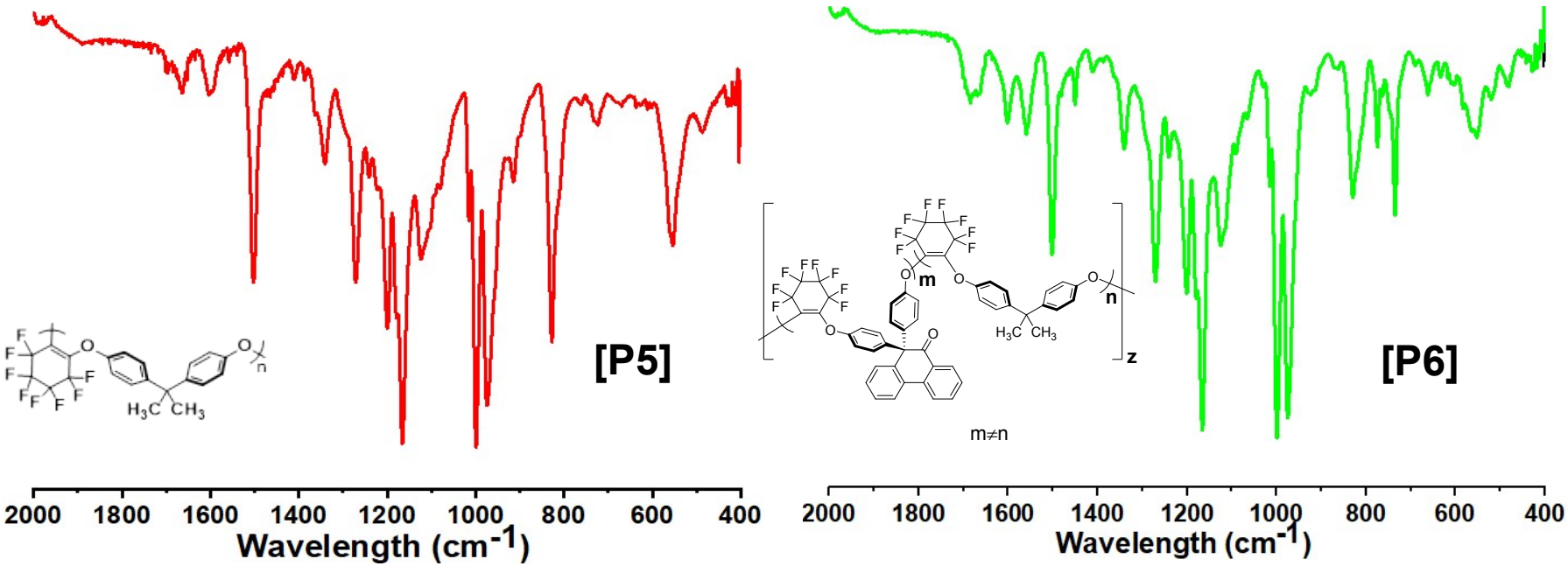

Figure S22. Fourier Transform Infrared analyses of polymers **P5-P6** between the wavelengths 2000-400 cm^{-1}.

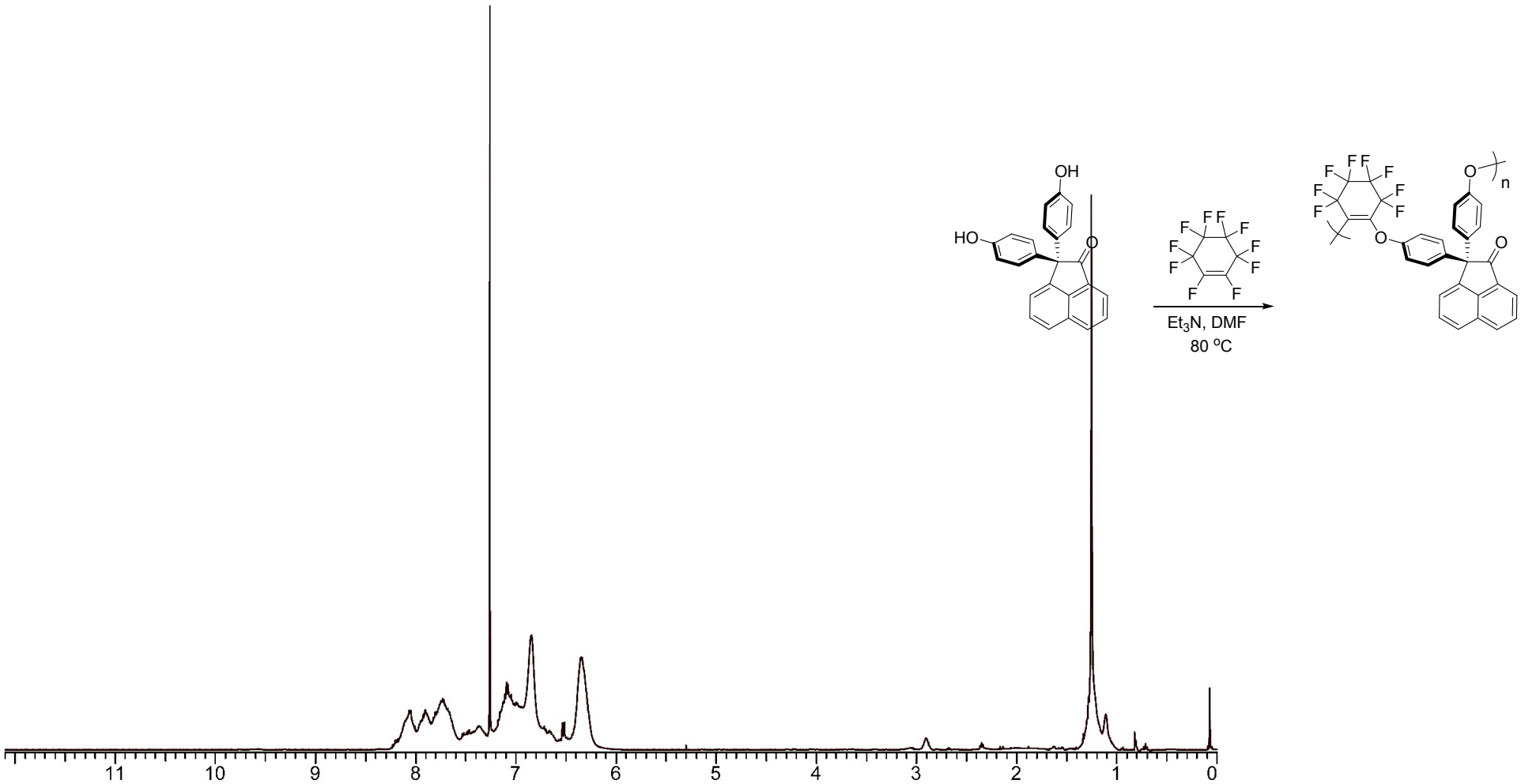
OH
HO
O
F F
F
F
F
F
F
F
F
F
Et3N, DMF
80 °C
O
n
O
O
11
10
9
8
7
6
5
4
3
2
1
0

Figure S23. ^{1}H-NMR spectra of **P1** in $CDCl_3$.

Figure S24. ^{13}C-NMR spectra of **P1** in $CDCl_3$.

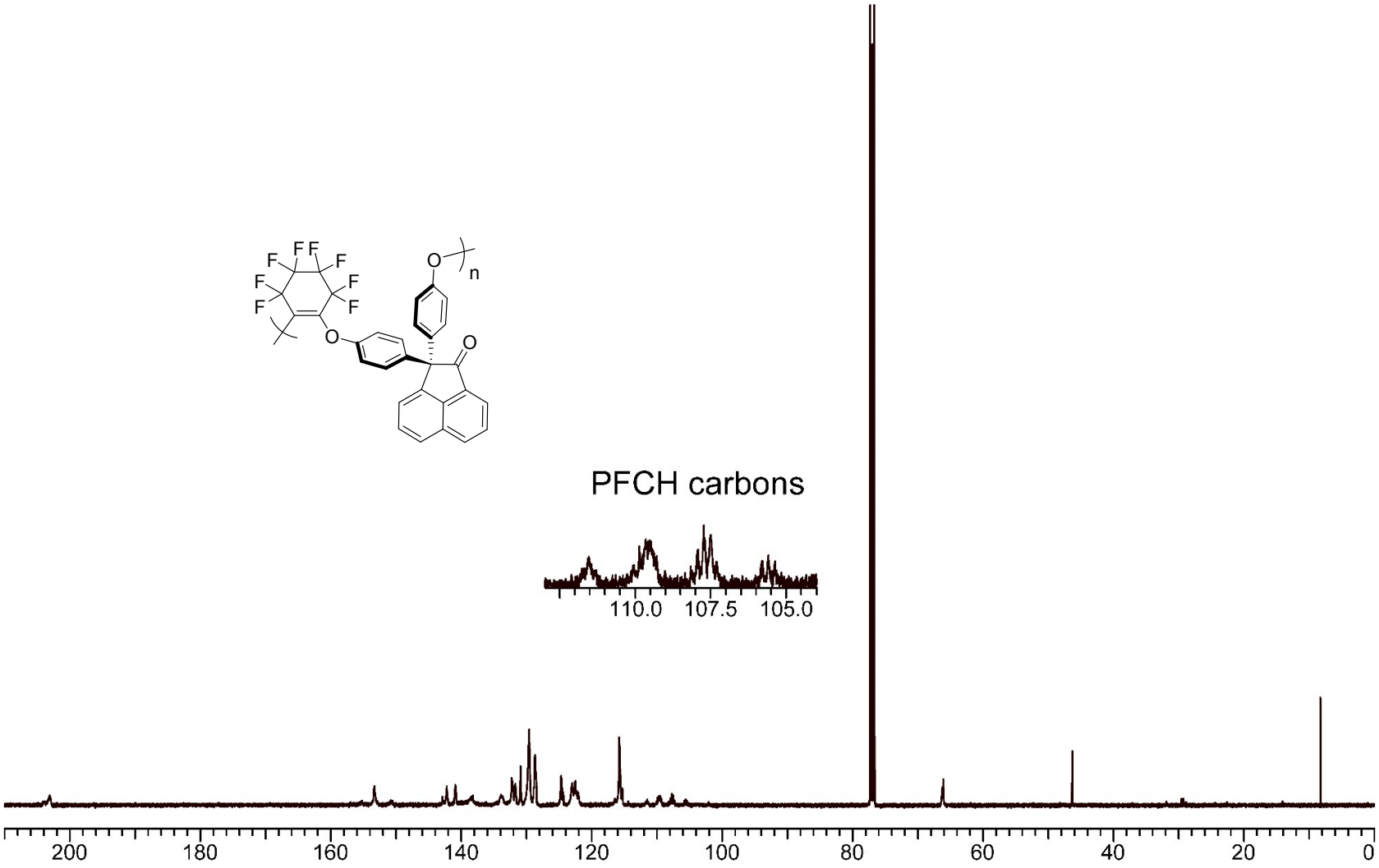

Figure S25. ^{19}F-NMR spectra of **P1** in $CDCl_3$.

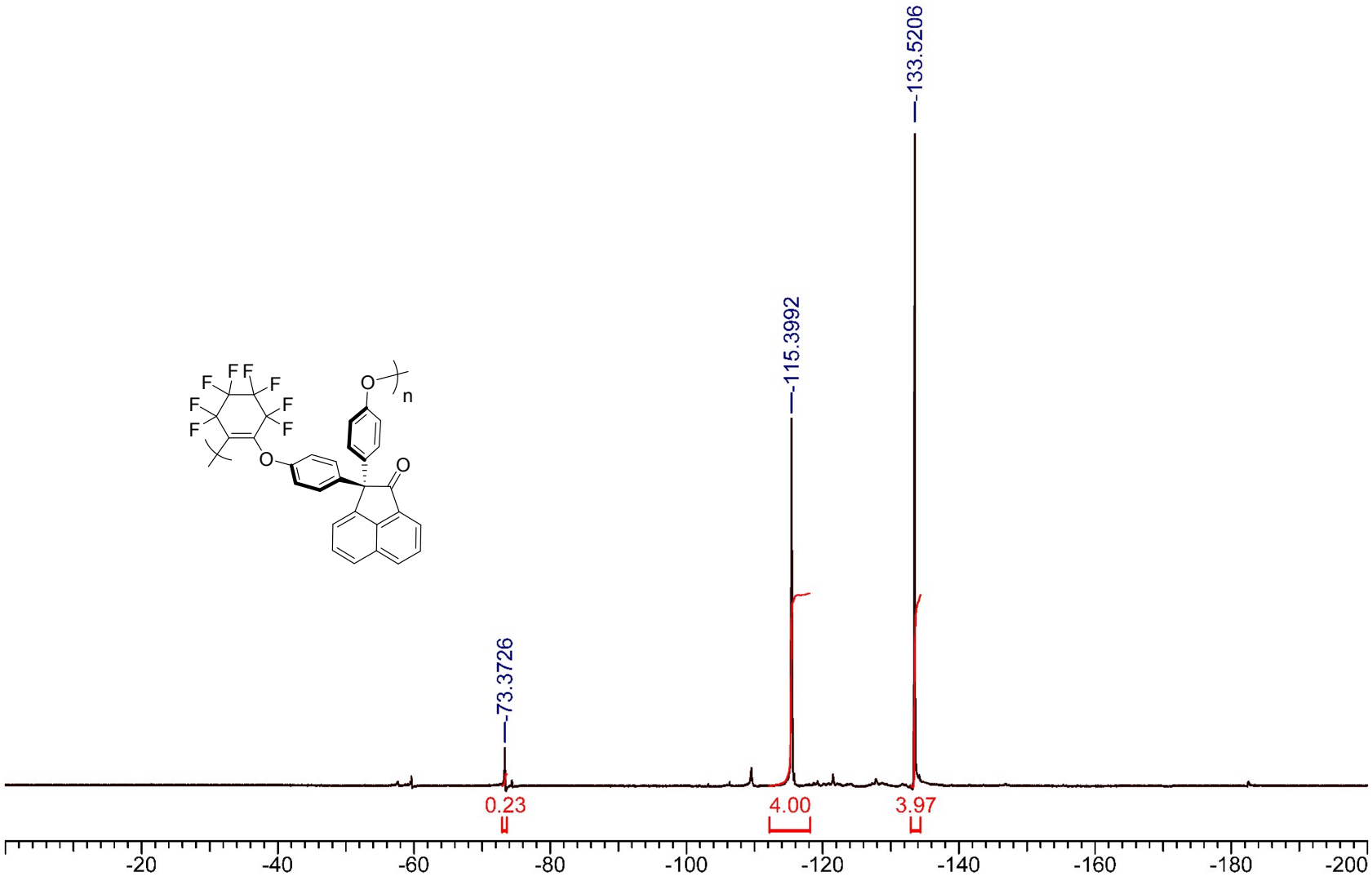

Figure S26. ^{1}H-NMR Spectra of **P2** in $CDCl_3$.

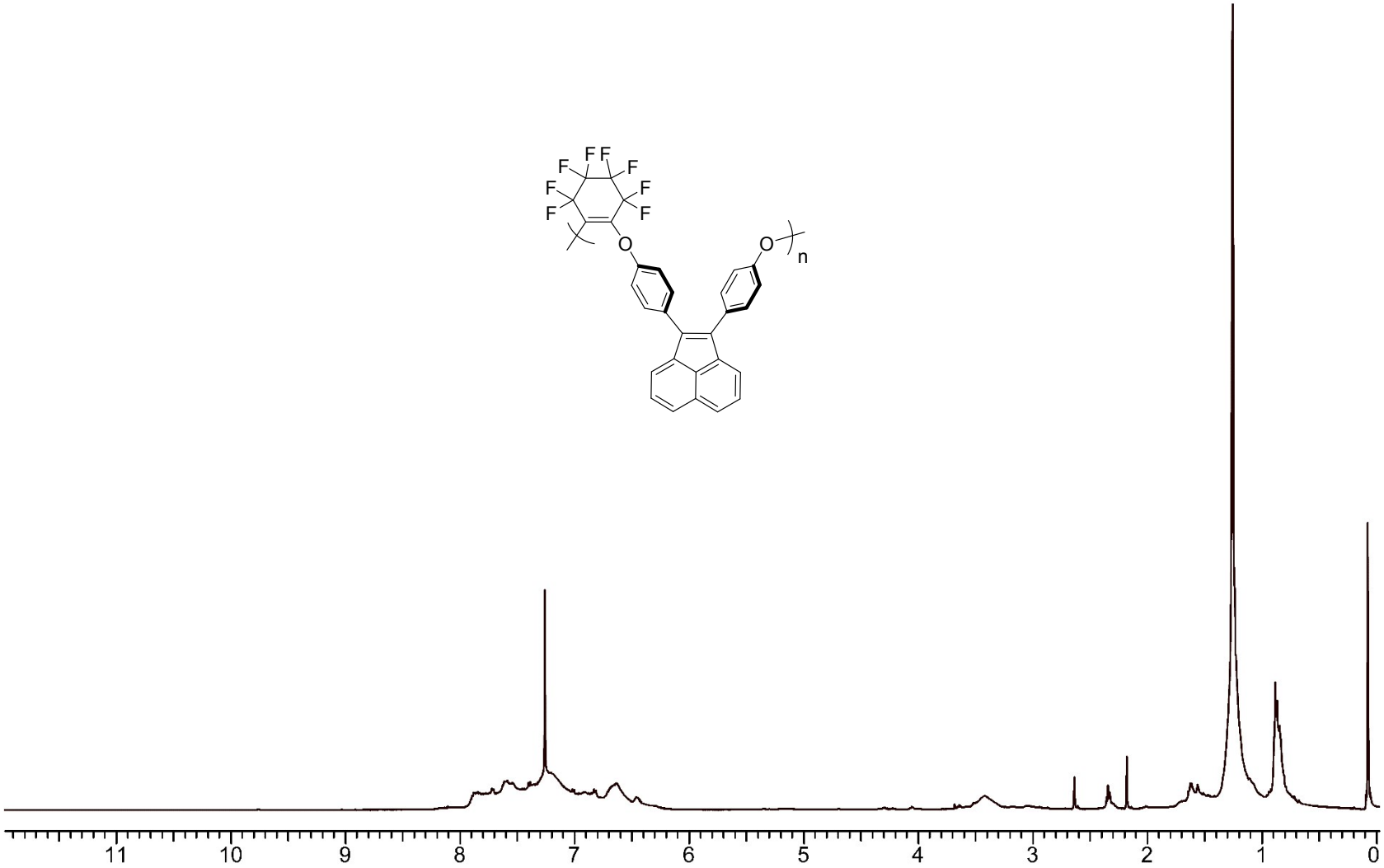

Figure S27. ^{19}F-NMR spectra of **P2** in $CDCl_3$.

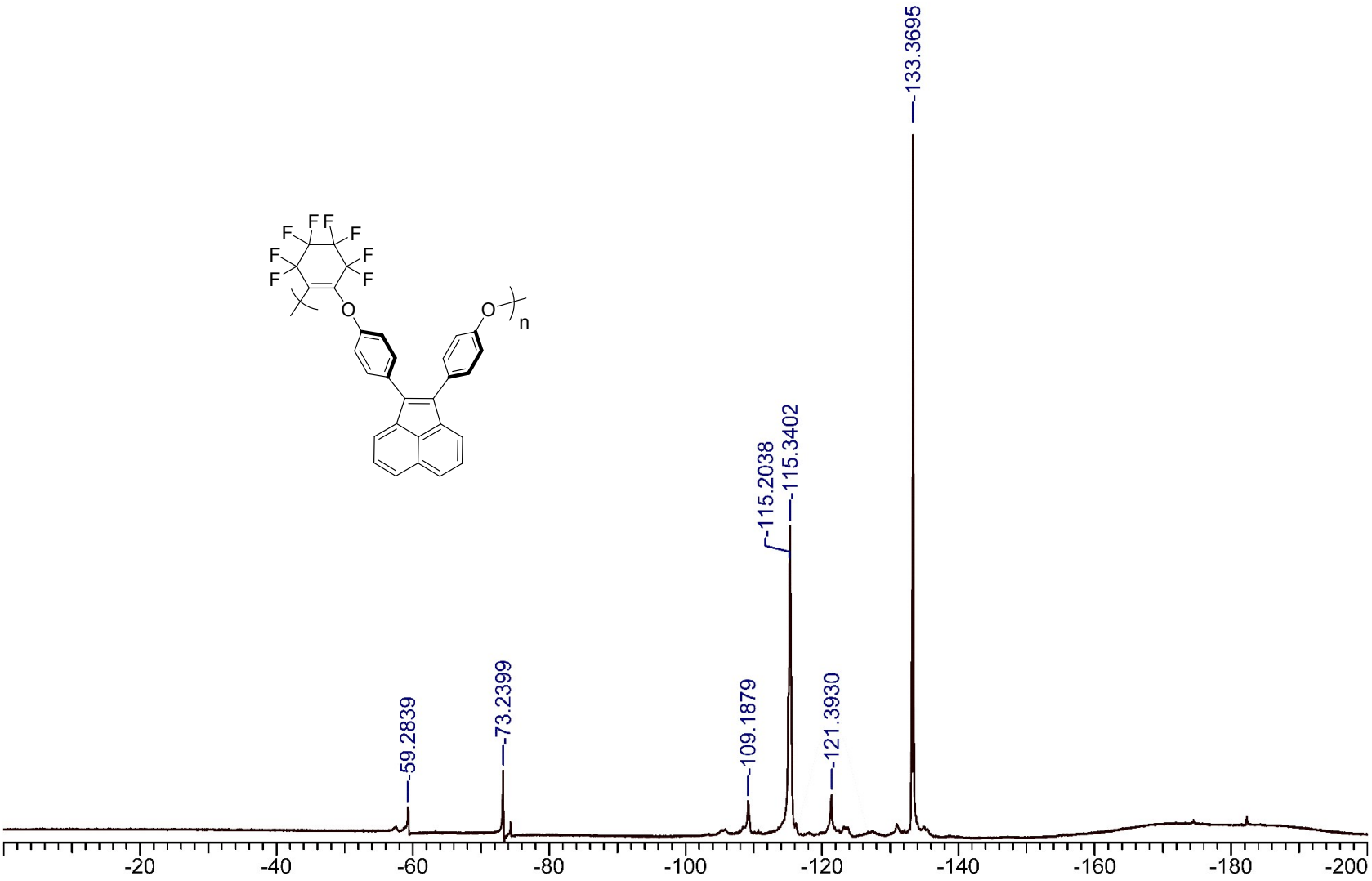

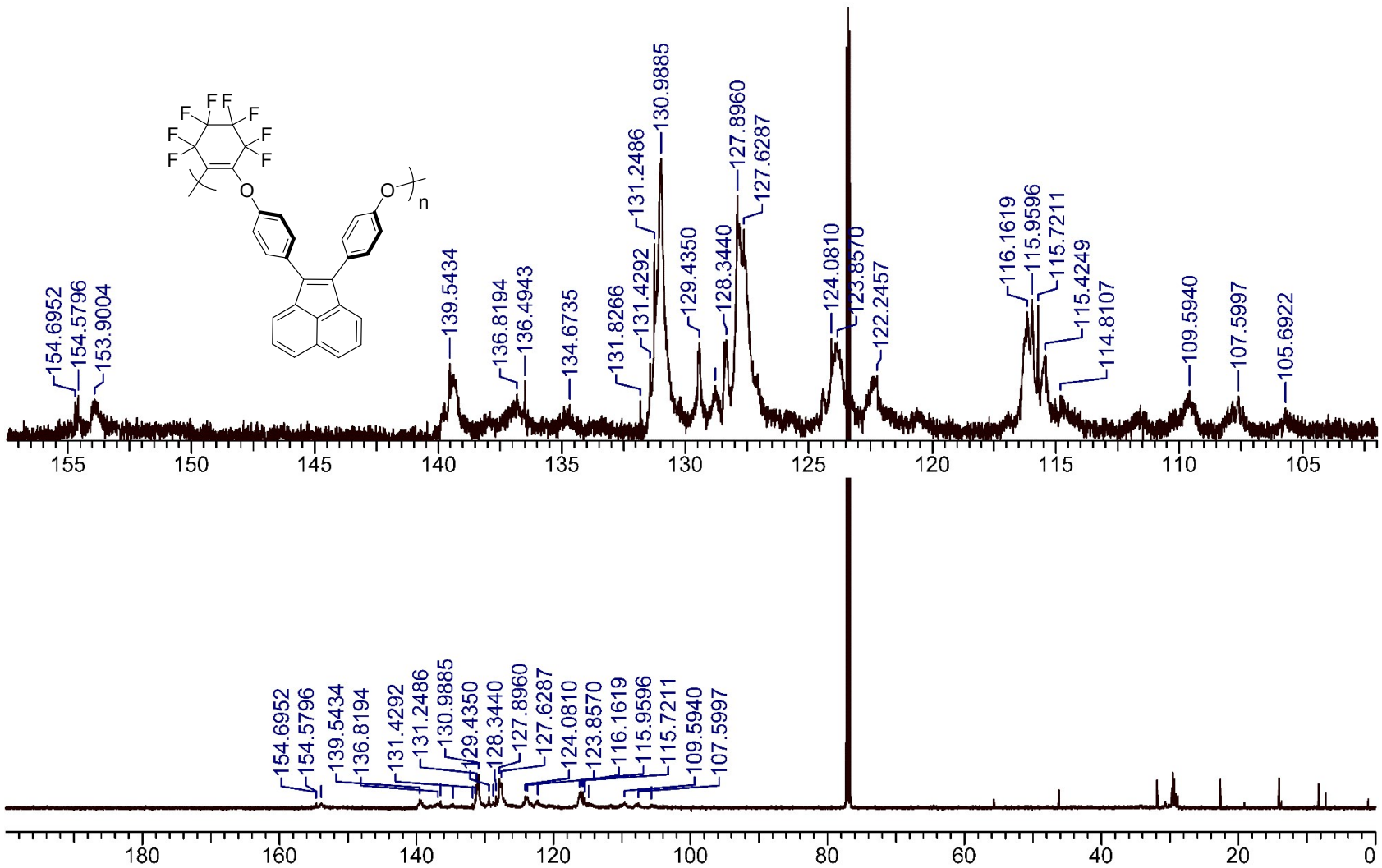

Figure S28. ^{13}C-NMR spectra of **P2** in $CDCl_3$.

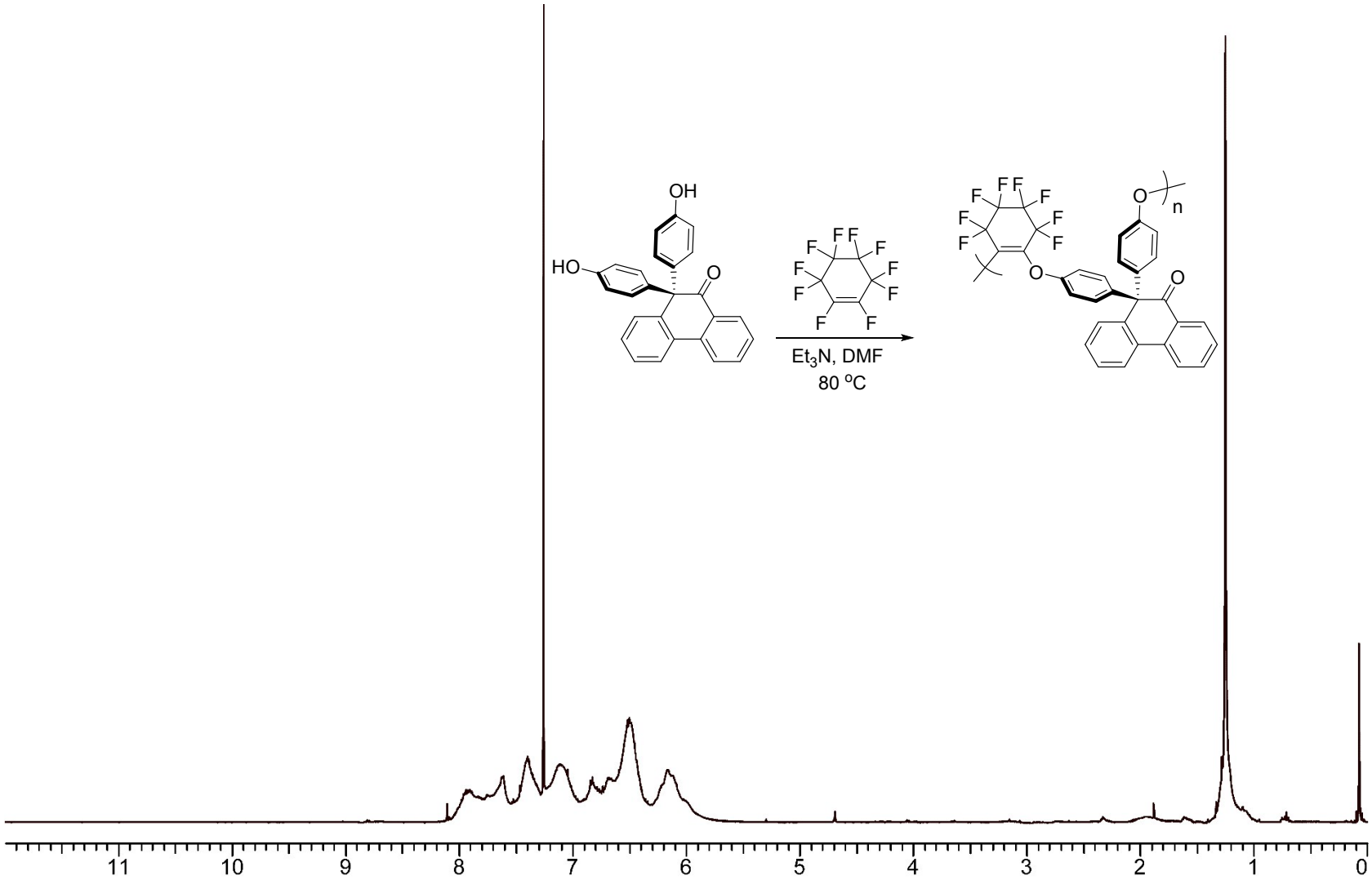

Figure S29. ^{1}H-NMR spectra of **P3** in $CDCl_3$.

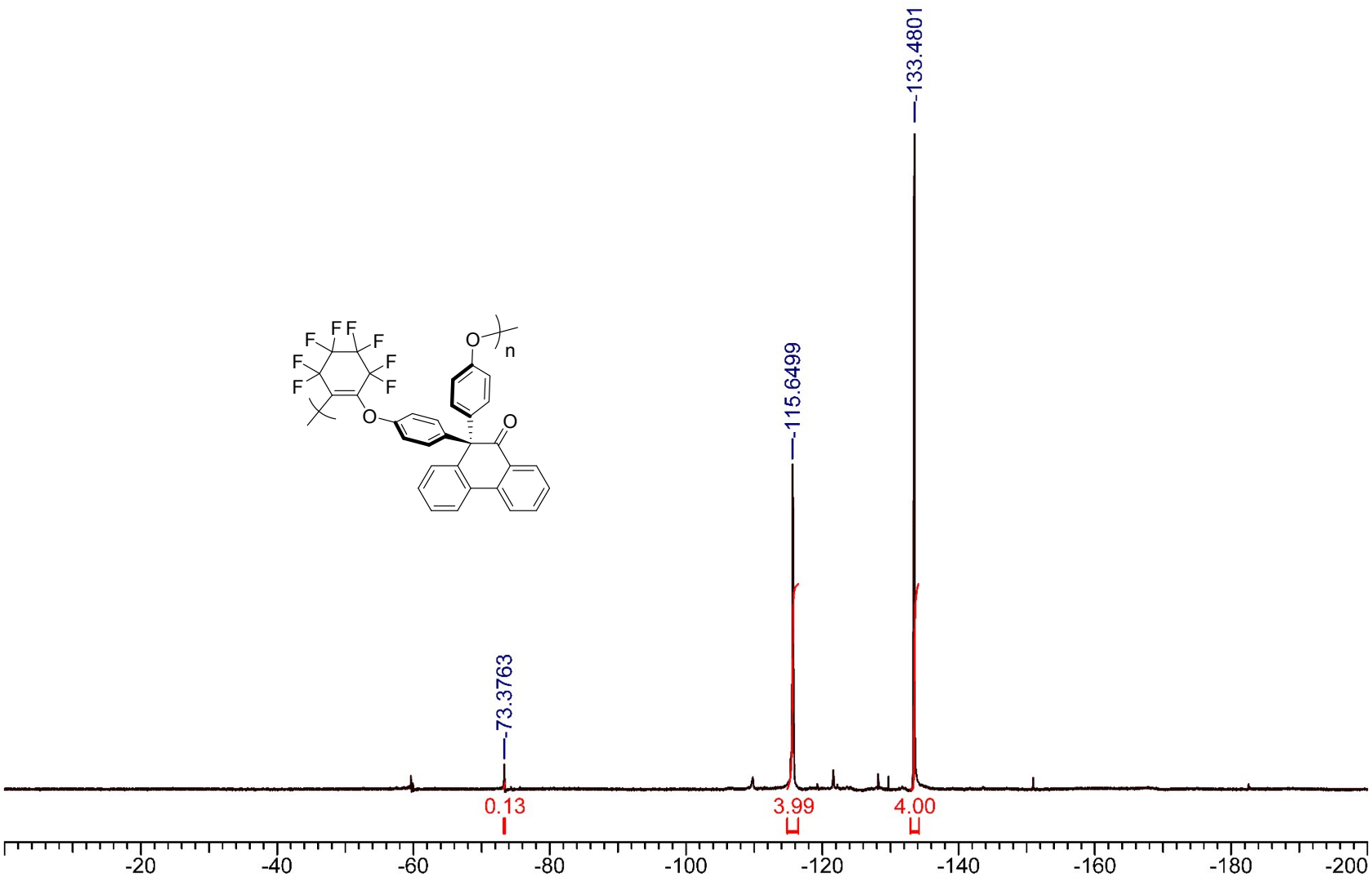

Figure S30. ^{19}F-NMR Spectra of **P3** in $CDCl_3$.

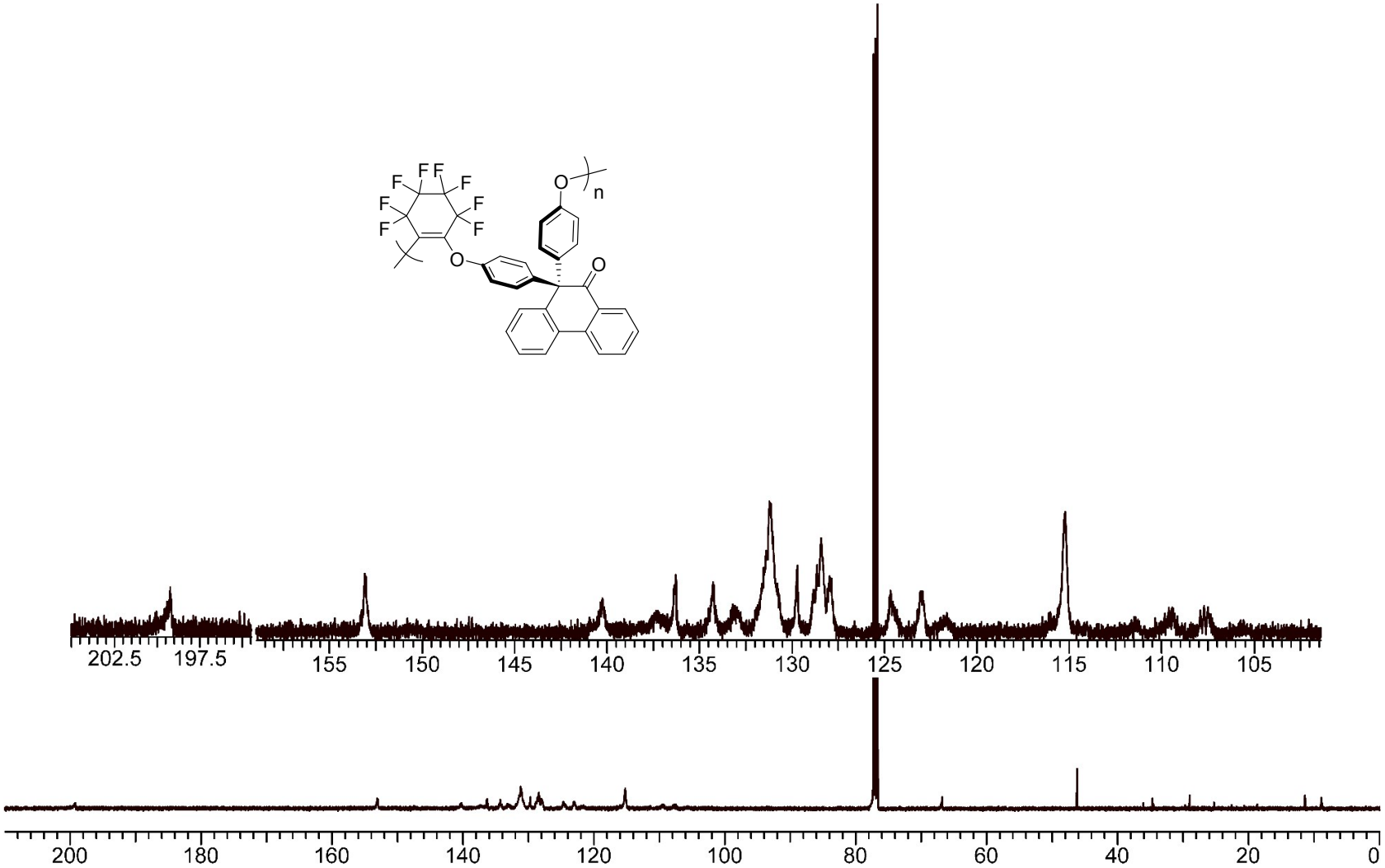

Figure S31. ^{13}C-NMR spectra of **P3** in $CDCl_3$.

Figure S32. ^{1}H-NMR spectra of **P4** in $CDCl_3$.

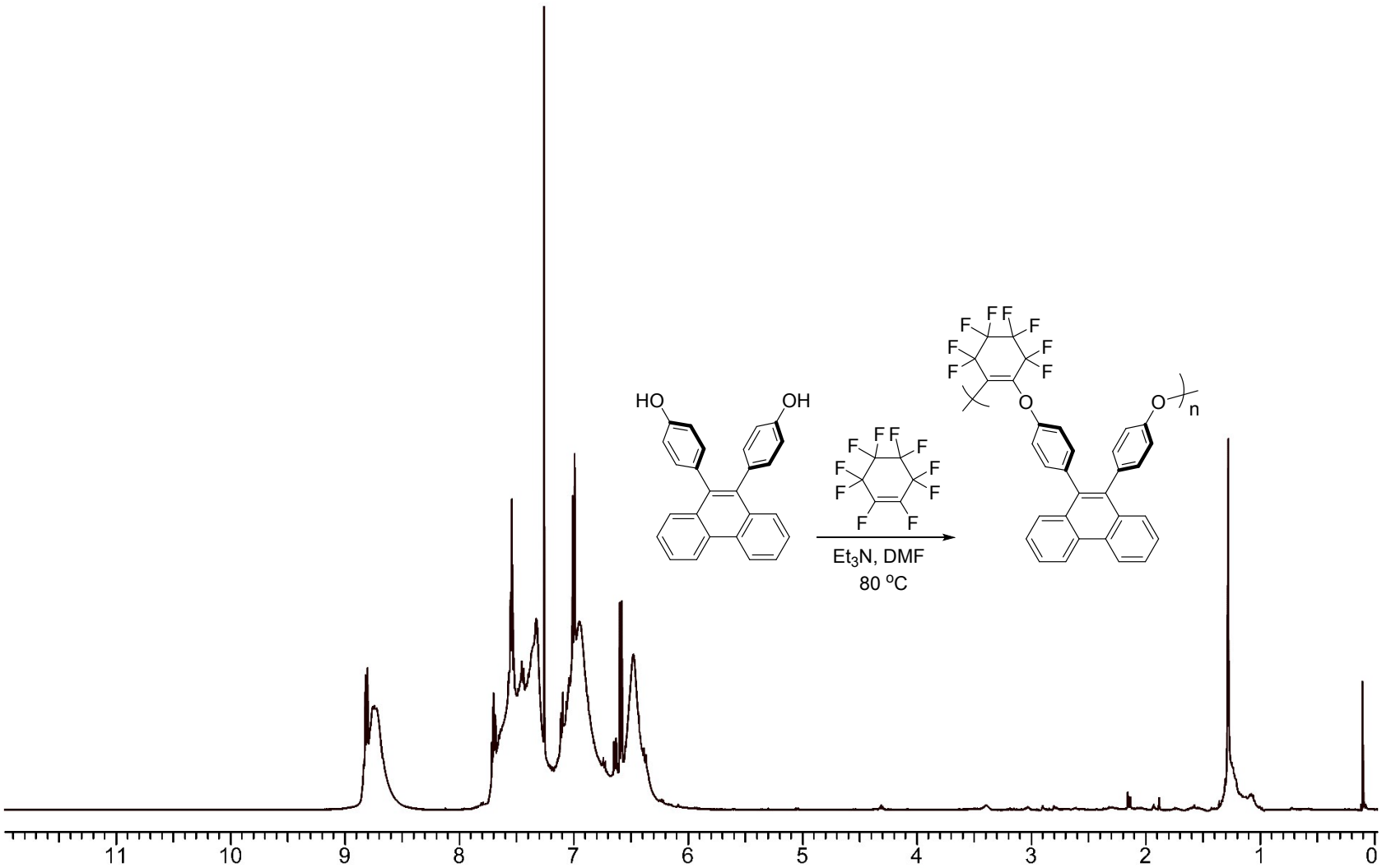

Figure S33. ^{19}F-NMR spectra of **P4** in $CDCl_3$.

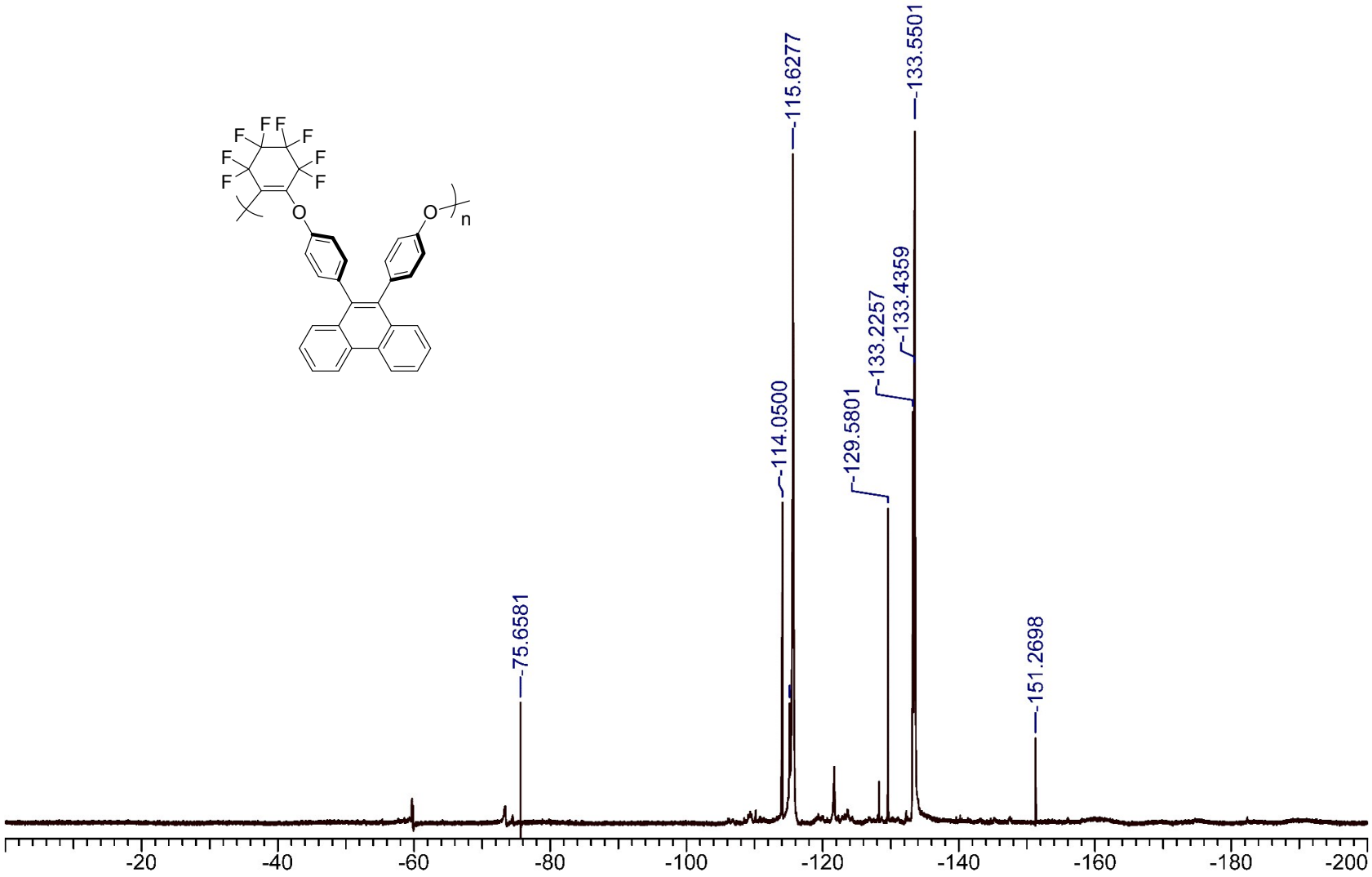

Figure S34. ^{13}C-NMR spectra of **P4** in $CDCl_3$.

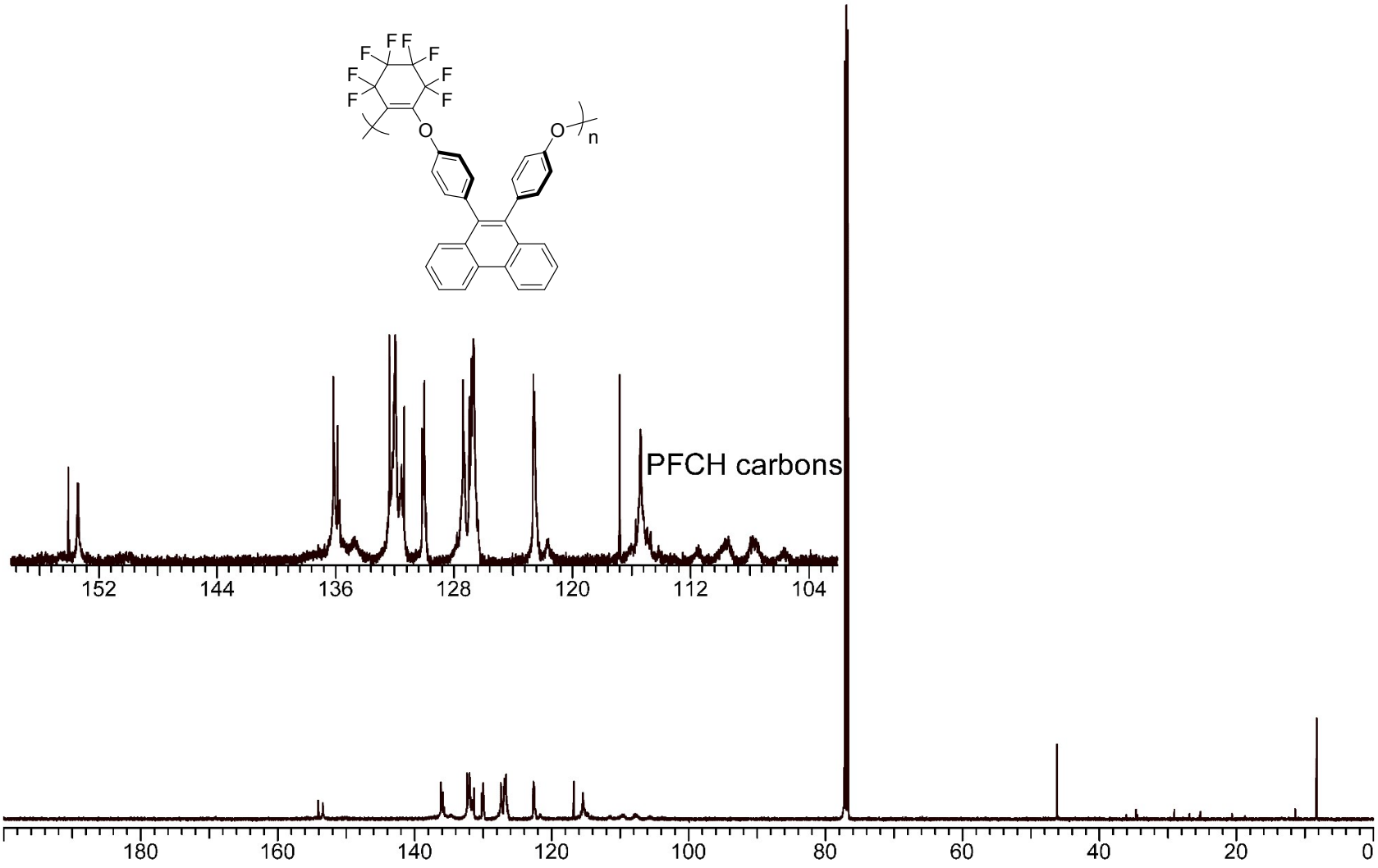

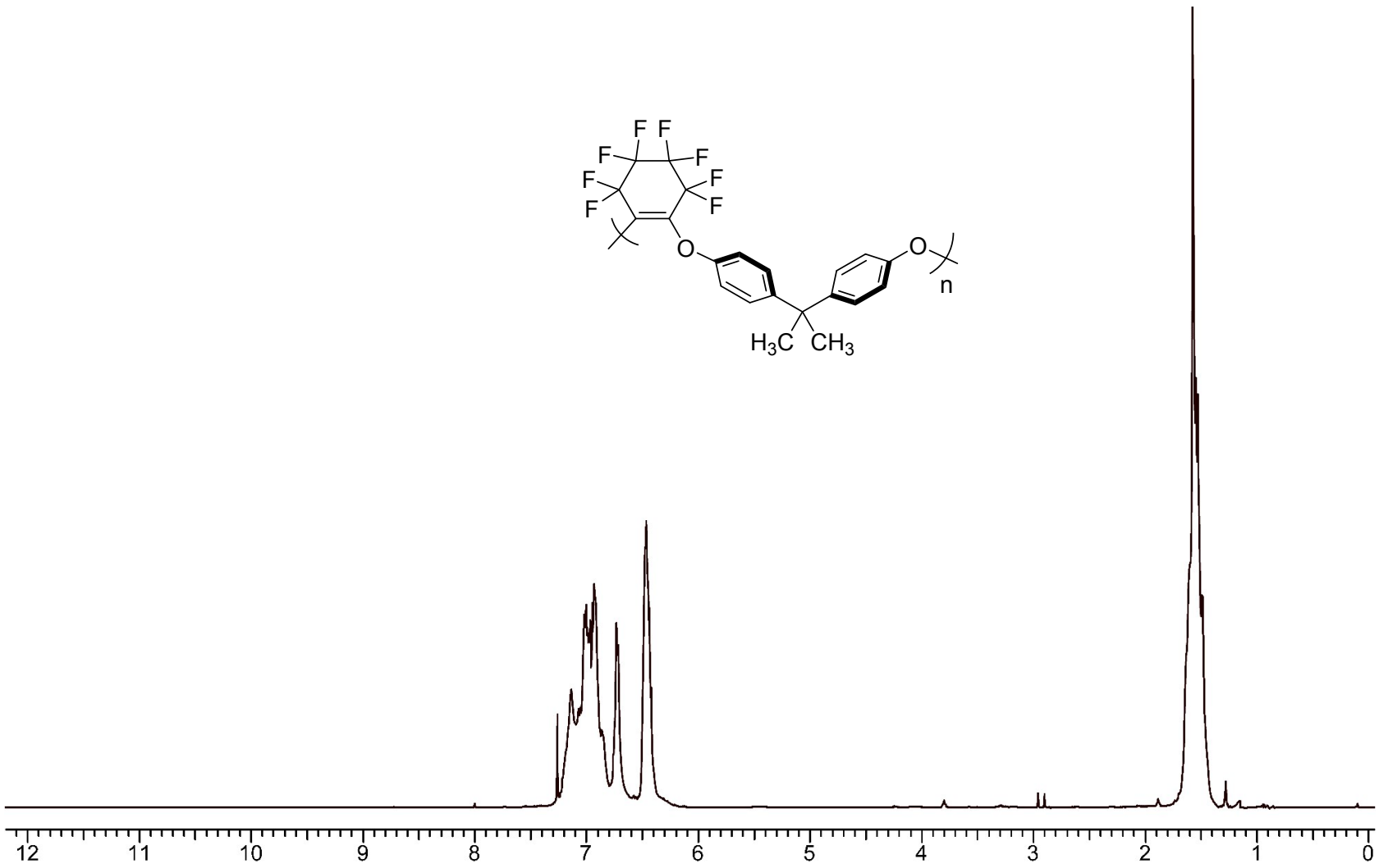

Figure S35. ^{1}H-NMR spectra of **P5** in $CDCl_3$.

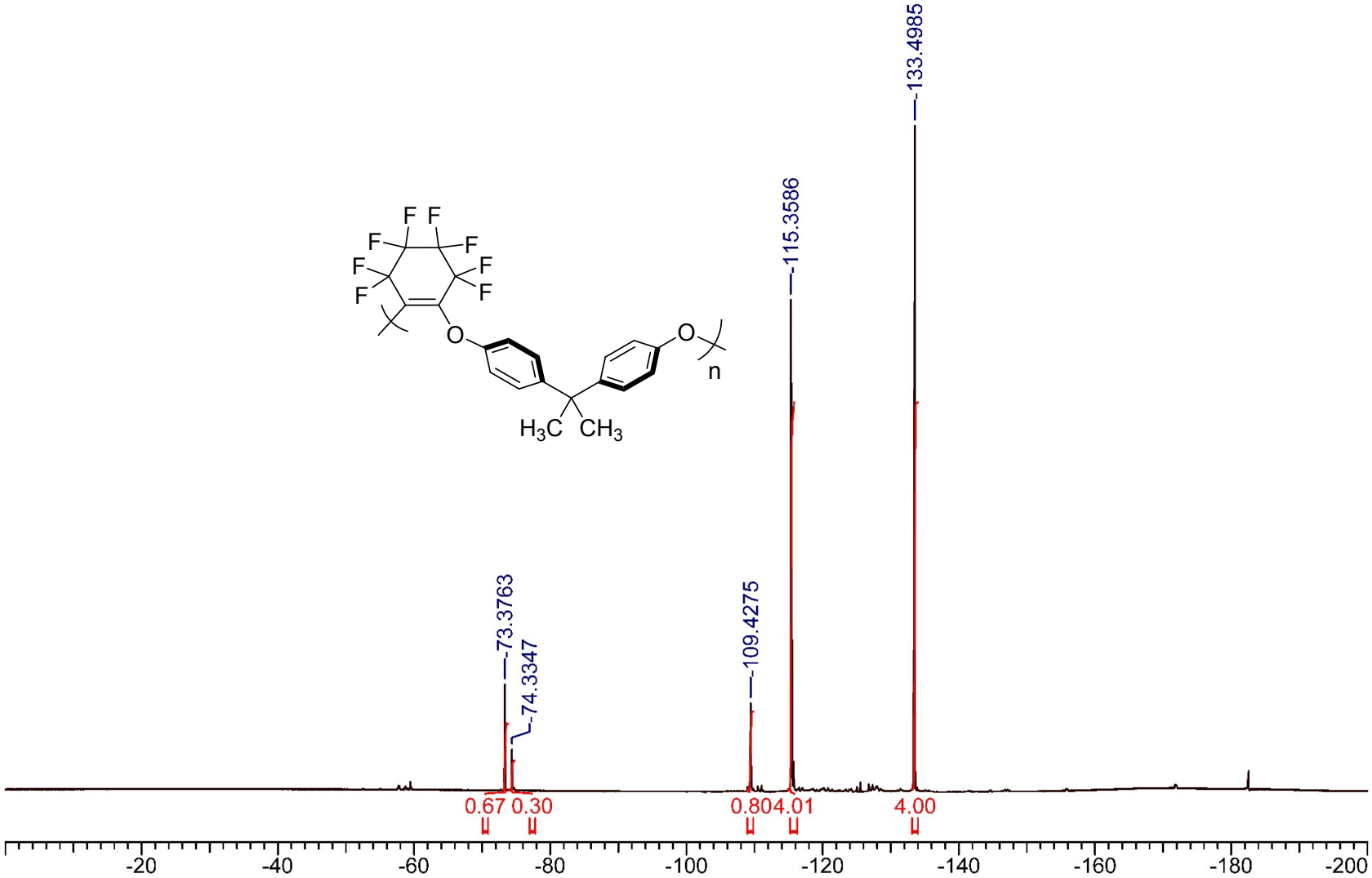

Figure S36. ^{19}F-NMR spectra of **P5** in $CDCl_3$.

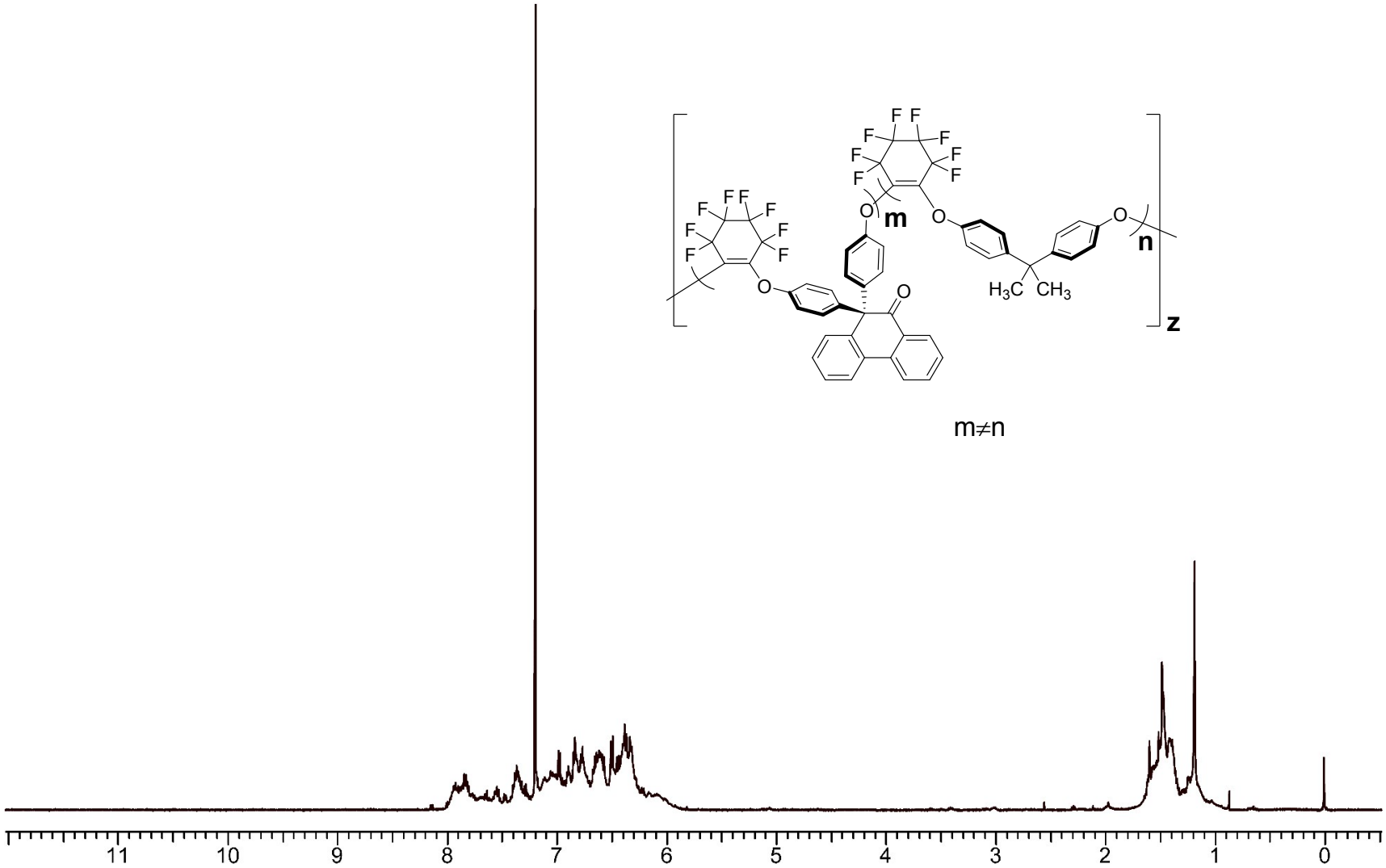
m≠n
m
n
z
11
10
9
8
7
6
5
4
3
2
1
0

Figure S37. ^{1}H-NMR spectra of **P6** in $CDCl_3$.

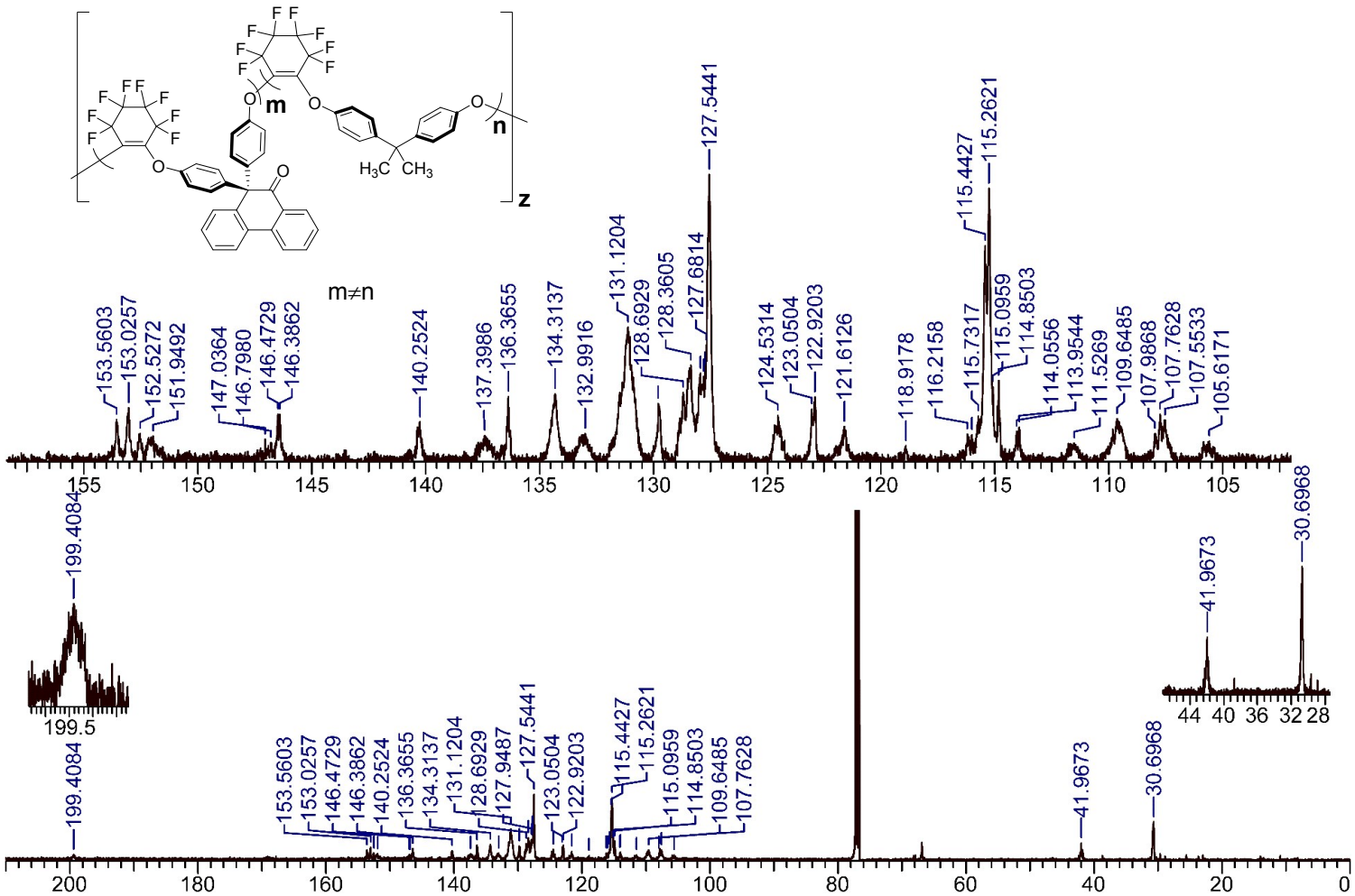

Figure S38. ^{13}C-NMR spectra of **P6** in $CDCl_3$.

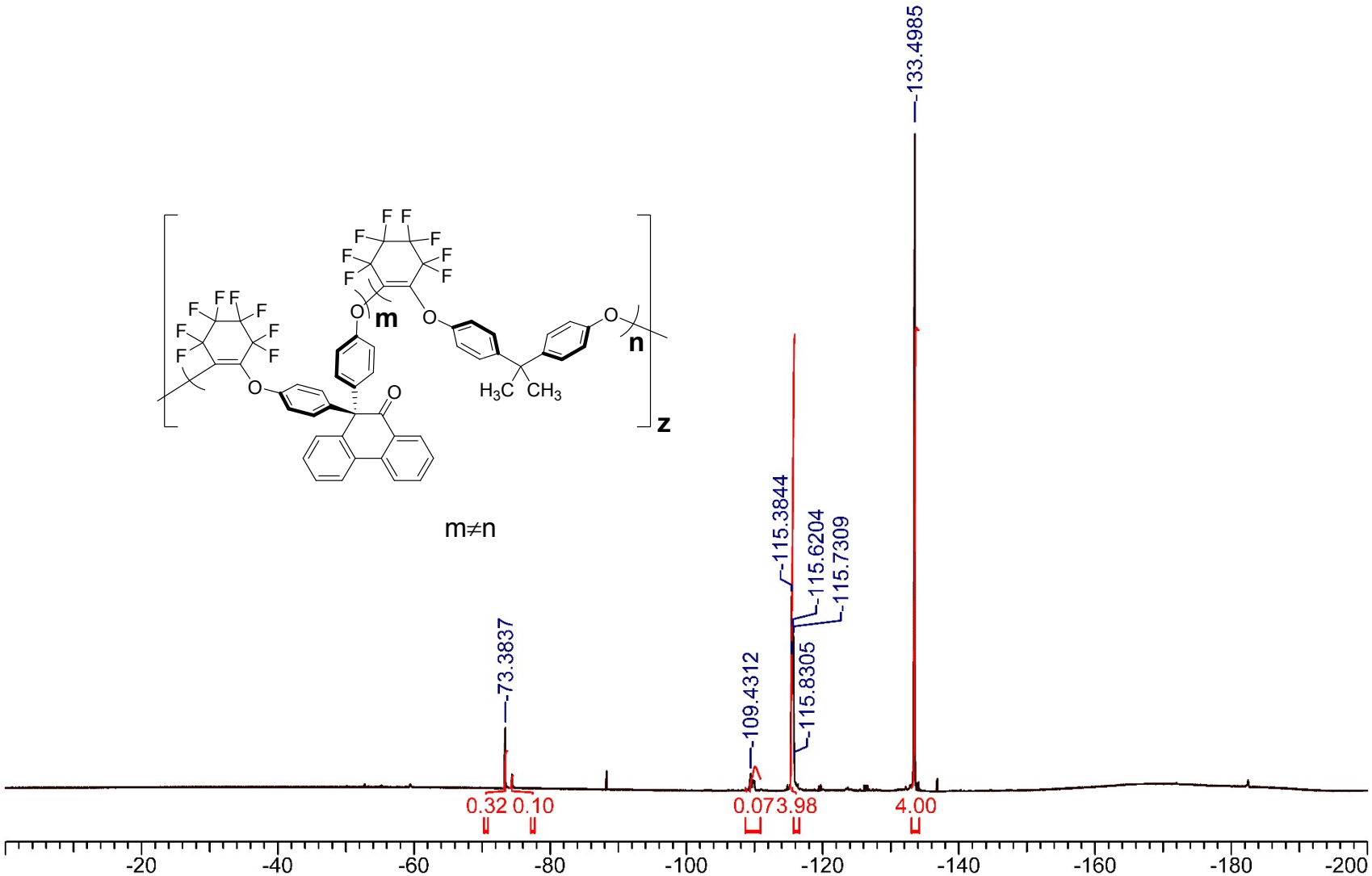

Figure S39. ^{19}F-NMR spectra of **P6** in $CDCl_3$.

References

S1. Motokawa, T.; Murase, H.; Yamada, M.; Miyauchi, S.; Minami, S.; Kuratani, H.; Shibayama, K. Manufacture of aromatic compounds with high heat resistance and high refractive index. JP 2011074012A. 2011.